UNIVERSITY OF CALIFORNA
RIVERSIDE

Biogeochemical Cycling in Costa Rica Margin Sediments as Recorded in Stable Sulfur Isotopes

A Thesis submitted in partial satisfaction
of the requirements for the degree of

Master of Science

in

Geological Sciences

by

Caroline Susanne Gott

June 2016

Thesis Committee:
Dr. Timothy Lyons, Chairperson
Dr. Natascha Riedinger
Dr. Sandra Kirtland Turner

The Thesis of Caroline Susanne Gott is approved:

_____

_____

_____

Committee Chairperson

University of California, Riverside

ACKNOWLEDGEMENTS

I would like to thank my advisor Prof. Tim Lyons for all of his support, encouragement, tremendous knowledge and guidance throughout my time at UCR. Since 2012, Tim has provided motivation and insight that have proven endlessly helpful.

Appreciation goes to Natascha Riedinger who has leant countless hours both in person and via Skype across time zones. Thank you Natascha for your mentoring, patience and pep talks.

Thanks also go to my third committee member, Sandy Kirtland Turner who provided a wealth of knowledge specific to IODP research as well as feedback on presentations and writing alike.

I thank fellow graduate students Konstantin Choumiline, Charles Diamond, Leanne Hancock, Dalton Hardisty, Bridget Lee and Stephanie Olson), lab manager (Steve Bates) and research technician (Andrew Robinson) for their collaboration and camaraderie. Thanks also to my office mate, Kelden Pehr for input and support.

I would like to acknowledge the Integrated Ocean Drilling Program (IODP) for collecting samples and Mike Formolo for making this work possible by making those samples available. Additionally, I express my thanks to Marta Torres for collaboration and insightful discussion.

Lastly, thank you to my family for always being supportive of my goals.

ABSTRACT OF THE THESIS

Biogeochemical Cycling in Costa Rica Margin Sediments as Recorded in Stable Sulfur Isotopes

by

Caroline Susanne Gott

Master of Science, Graduate Program in Geological Sciences
University of California, Riverside, June 2016
Dr. Timothy Lyons, Chairperson

The complex sedimentary and tectonic interactions of the Costa Rica margin have had a poorly understood impact on biogeochemical cycles. Although it is known that continental margins feature high rates of sulfate reduction and fluid flow within sediments, the biogeochemical limits of such environments are not well known. In this research, I focused on sulfur geochemistry from sediments collected during the Integrated Ocean Drilling Program (IODP) Expedition 344 at Holes U1381C, U1413B and U1414A. The goal of this research was to investigate the dynamic biogeochemical processes of this complex system, particularly the sulfur cycle, and to explore how these processes are recorded in the geologic record.

The examined sediments indicated biological sulfur cycling in several ways. Sediments at Hole U1381C show signs of microbial reduction of sulfate, with

depleted sulfate concentrations and heavy sulfate-S isotope offsets relative to Vienna- Canyon Diablo Troilite (V-CDT) ($\delta^{34}S$ >+70 ‰). However, the product of this reaction, H_2S, is notably absent from the pore waters. The sediments of Hole U1413B are characterized by a shallow (~15 mbsf) sulfate-methane transition zone (SMT) where released hydrogen sulfide reacts with reactive iron to form iron sulfides. In contrast, in Hole U1414A pore water sulfate is still present several hundreds of meters below the seafloor, hydrogen sulfide concentrations are low (<4 μM). Sequential extractions of iron oxides reveal the presence of reactive iron phases, although in low concentrations, at hundreds of meters of depth (< 1.1 wt.%). The presence of reactive iron minerals in the deep sediments at Hole U1414A has implications for the biosphere through the persistence of microbially available electron acceptors at great depth.

The extreme pore water sulfur isotope ratios observed here are expressed in sulfate $\delta^{34}S$ values that reach up to +140 ‰. I used Rayleigh modeling to find the fractionation factor (α) of the most isotopically heavy sulfates to compare to known values for various drivers of sulfate isotope enrichments. It was found that the unprecedented isotopically heavy sulfate is likely biological in origin and the unique setting may be the clue to expanding what is known about the boundaries of biologically induced fractionation.

TABLE OF CONTENTS

LIST OF FIGURES

LIST OF TABLES

1. Introduction

1.1 Biogeochemistry of Sulfur Cycling

Sulfur, an essential component of amino acids for protein building in both eukaryotes and prokaryotes, is among the most biologically important elements (Reisner, 1956; Cooper 1983; Brosnan and Brosnan, 2006). Bioavailable sulfur—that is, phases readily utilized for metabolic processes—can be found in multiple forms including elemental sulfur, sulfide, and sulfate (Ammerman et al., 1994; Shen et al., 2013). Given its broad importance, this research focuses on the sulfur cycle

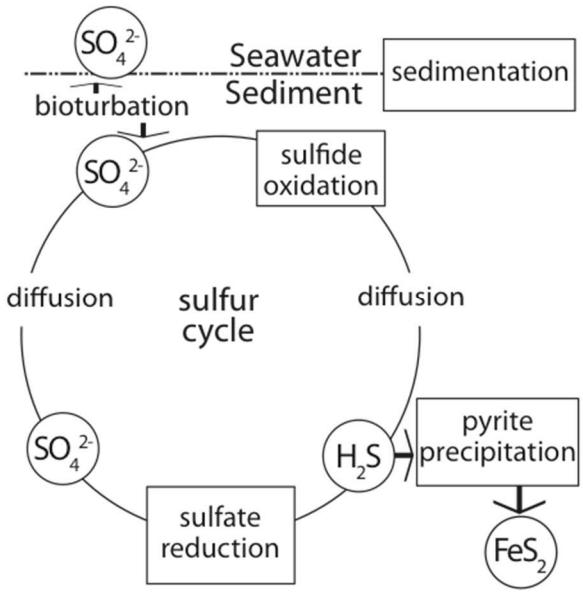

Figure 1. Sulfur cycle in marine Sediments. Figure modified from Jørgensen 1979. Cycle shows both abiotic and biotic aspects of the sulfur cycle in marine sediments.

within marine sediments. In a marine sediment setting, microbes reduce sulfate forming hydrogen sulfide, which can accumulate in sediments, diffuse through the sediment, or react with metals to form metal sulfides—in particular through reaction with iron to form pyrite (see Figure 1). Accumulation of measurable pyrite therefore is dependent on both ample supplies of sulfide and reactive iron, which

demands that iron should be measured alongside sulfur compounds. Furthermore, the steps of bacterial sulfate reduction link sulfur to the cycles of carbon (via microbial decomposition of organic matter) and oxygen (through the burial of reduced S) in marine environments (Berner, 1982; Garrels and Lerman, 1984).

In many biotic and abiotic chemical reactions, light isotopes of elements are known to be preferentially depleted in the parent reservoir, often resulting in pronounced isotopic offsets (fractionations) between parent and product compounds. Bacterial reduction of sulfate and the resultant depletion of the lighter S isotope is a prime example of biologically fractionated isotopes (Goldhaber and Kaplan, 1974; Kendall and Caldwell, 1998). Among the stable isotopes of sulfur, the two most abundant in nature are ^{34}S and ^{32}S (Thode 1970), and they are the focus of this study. During bacterial sulfate reduction, the lighter isotope ^{32}S is preferentially depleted in the sulfate pool as sulfide is formed, leaving the remaining sulfate pool comparatively isotopically heavier. Similarly, as the isotope mass balance demands, the sulfide formed during bacterial sulfate reduction is correspondingly enriched in ^{32}S compared to sulfate. In related discussions, the ratio of heavy to light isotopes in a given sample is normalized to a known standard for the purpose of comparisons among samples (see equation 1). The standard used to determine relative abundance of ^{34}S and ^{32}S is V-CDT (Vienna- Canyon Diablo Troilite). By measuring the isotope ratio of sulfate in the pore waters of marine sediments, we can explore the biological contribution to sulfur cycling in diverse marine and nonmarine settings (Kendall and Caldwell 1998).

$$\delta^{34}S = \left[\left(\frac{\frac{^{34}S}{^{32}S}_{sample}}{\frac{^{34}S}{^{32}S}_{V-CDT}} \right) - 1 \right] \times 1000$$

Equation 1.

In addition to their isotopic fingerprints, microbial metabolic processes yield other signatures that can be measured in sediments. One obvious expression of sulfate reduction is the decreasing amount of sulfate in pore waters as microbes reduce it to hydrogen sulfide. In any given marine sedimentary profile, there is typically a sequence of microbial metabolisms dictated by the availability of electron acceptors progressing from oxygen, nitrate, manganese, iron, and sulfate (Keys et al. 1935; Redfield, 1958; Orcutt et al. 2011). This hierarchy reflects the progression with increasing sediment depth from the most to least energetically favorable compounds for metabolizing organic matter. In oxygenated horizons, aerobic respiration is the most prevalent redox reaction. However, because sulfate is abundant in seawater (~28 mM), sulfate reduction contributes significantly to the total amount of organic degradation in many marine settings because typically, nitrate and metals are rapidly depleted (Orcutt et al., 2011). In this hierarchy, sulfate reduction is followed by methanogenesis. The shift between the metabolic dominance of sulfate reduction to methanogenesis, and more specifically the shift in chemical abundance is particularly relevant to this research and is commonly

referred to as the sulfate-methane transition (SMT) (Reeburgh, 1971; Iversen and Jørgensen, 1985).

$$2\,CH_2O^- + SO_4^{2-} \rightarrow H_2S^- + 2\,HCO_3^- \quad \textbf{Equation 2.}$$

Immediately above the SMT (in regions that have a well defined transition), sulfate is abundant and sulfate reduction is a principal source of energy for microbes that decompose organic matter, while converting sulfate to sulfide (see equation 2) (Berner, 1989). Organic matter is required as the electron donor as sulfate is reduced to sulfide and reduced C is oxidized to DIC (dissolved inorganic C) (Berner, 1985; Fossing et al., 2000). Based on the above equation, sediments dominated by sulfate reduction should not only be depleted in sulfate but should also contain abundant sulfide unless it is removed via diffusion or reacts with a metal such as iron.

1.2 Bacterial sulfate reduction and alkalinity

Total alkalinity is linked to the biogeochemical cycling of sulfate by increasing (principally through the production of bicarbonate) as both sulfate and organic matter are consumed (Wolfe-Gladrow et al. 2007). This observed relationship between sulfate, TOC, and alkalinity is another chemical expression of microbial activity; however, microbial sulfate reduction is not the only control on alkalinity. Alkalinity is also strongly tied to calcium carbonate chemistry through

dissolution and precipitation, and a decrease of dissolved calcium typically corresponds to an increase in alkalinity (Tsunogai et al., 1973; Horibe et al., 1974; Tsunogai and Watanabe, 1981).

1.3 Review of Sulfur Isotope Fractionation in Marine Sediments

The sulfate-S isotope composition of ocean water is uniformly about +20‰ (Szabo et al., 1950; Thode et al, 1961; Rees et al., 1978) but the associated sulfate isotope fractionations in marine systems can vary widely from this baseline (Holser and Kaplan, 1966; Strauss, 1997; Detmers et al., 2001). Numerous factors control the extent of biological fractionation of sulfate, including temperature, pressure, the amount and type of organic matter present, and rate of sedimentation in a given region, all of which affect the rate of sulfate reduction, as well as the amount of sulfate present (Goldhaber and Kaplan, 1982; Westrich and Berner, 1984; Habicht and Canfield, 1997). Increases in the $\delta^{34}S$ of sulfate relative to the average seawater value are often indicative of microbial reduction. It is typical for S fractionation in marine sediments to measure between +30‰ and +50‰, although much higher values are also observed (Holser and Kaplan, 1966, Habicht and Canfield, 1997). Based on experimental work, it was previously thought that biologically induced sulfate fractionation in ocean water or marine sediment pore waters could go no higher than $\delta^{34}S\text{-}SO_4$=+46‰ (Kaplan and Rittenberg, 1964). Since that work, however, additional research has demonstrated the potential for much higher

fractionations via sulfate reduction alone (Canfield et al., 2010; Sim et al., 2011)). Pore water sulfate isotope ratios considered to be heavy yet common can range up to +70-72‰ (Goldhaber and Kaplan, 1980; Strauss 1997, Canfield and Teske, 1996, Wortmann et al., 2001). Notable outliers are biologically induced fractionation factors as low as 2‰ (Detmers et al., 2001) and the very high value of $\delta^{34}S$-SO_4=+135‰ found in the Cascadia Basin (Rudnicki et al., 2001).

In general, continental margins are characterized by greater rates of sulfate reduction relative to deeper portions of the ocean (Jørgensen, 1982; Canfield, 1991)—in part reflecting the greater availability of reactive organic phases, although the full range of controls is not well defined. Low rates of sulfate reduction (those with high fractionation factors) have been associated with heavier sulfate isotope ratios (Bottrell and Raiswell, 2000). There have been attempts to determine whether continental margins are host to unique microbial communities that may drive this increased sulfate reduction, but no distinctive diversities or abundances have been observed in the sediments of such study sites (Harrison et al., 2009). The research presented here can serve to to determine the upper limit of fractionation driven by microbial sulfate reduction and the associated controls.

1.4 Rayleigh Isotopic Fractionation

In addition to the chemical measurements listed above, mathematical modeling provides an additional perspective on the patterns and magnitudes of S fractionation during microbial sulfate reduction. Once the magnitude of

fractionation is quantified, one can better establish the environmental and biological controls under both steady- and nonsteady-state conditions by comparing calculated fractionation factors with those found other studies of sulfate isotope enrichments.

Known sulfate concentrations and $\delta^{34}S$ values can be used along with the Rayleigh equation to calculate the fractionation factor (See Equation 3) (Hayes, 2004), where R_R is the isotope ratio measured, R_o is the initial isotope ratio of the system, ƒ is the concentration at depth divided by the initial concentration, and ε represents the fractionation factor needed to produce the measured isotope ratio.

$$f^{\varepsilon_{P/R}} = \frac{R_R}{R_{R,O}} \textbf{ Equation 3.}$$

Alternatively, we can use a simplified form of the equation. Specifically, ranges of fractionation factors can be fit to known data sets (Hayes, 2004), as can be seen in Equation 4 where R has been replaced with $\delta^{34}S$.

$$\delta^{34}S_t = \delta^{34}S_O + \varepsilon \cdot \ln f \textbf{ Equation 4.}$$

Finally, our calculated fractionation factors can reported in terms of alpha rather than epsilon for the purpose of directly comparing our findings to those of other research. The relationship between epsilon and alpha can be seen in Equation 5.

$$\varepsilon = (\alpha - 1) \times 1000 \textbf{ Equation 5.}$$

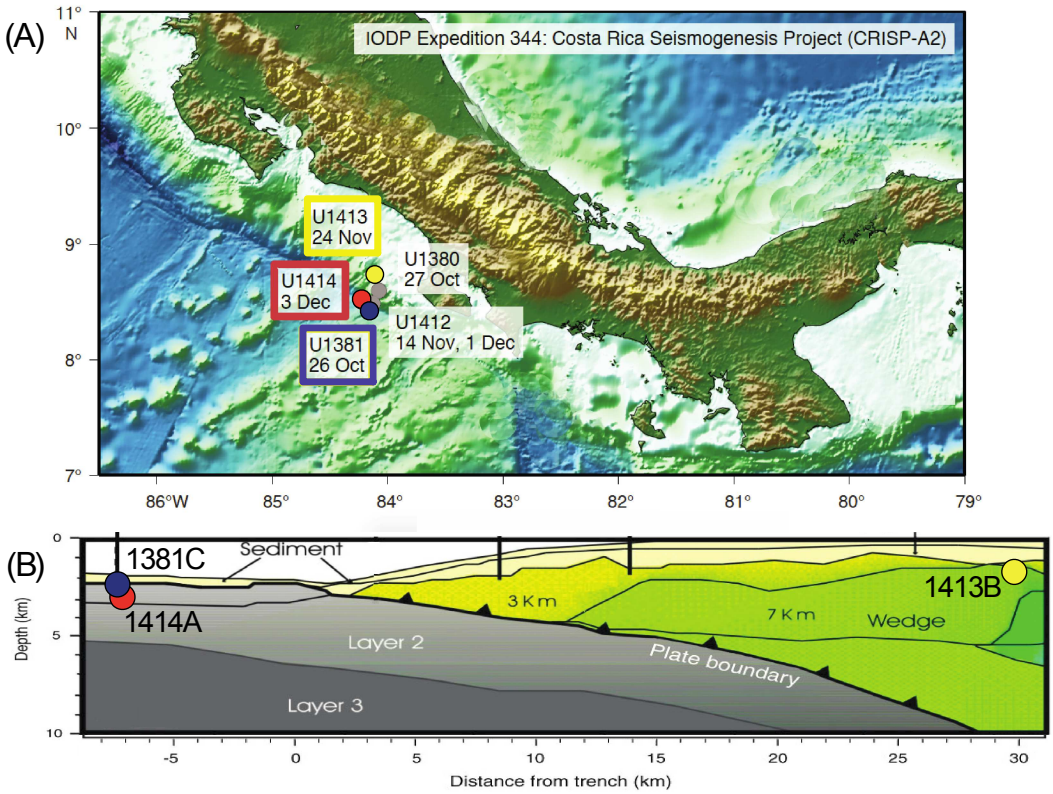

Fig 2. Sample location and core proximity to trench.
(A) Map of sampling sites for IODP Expedition 344. All samples were taken off the west coast of Costa Rica. Also shown are the dates each site was sampled. Dates shown are all in 2012 (Expedition 344 Scientists, 2013b). (B) Cores used in this study depicted in relation to the subduction plate. The grey shaded plate to the left of the plate boundary is the subducting Cocos plate. The overlaying green plate is the Caribbean plate (modified from Stavenhagen et al., 1998).

1.5 Sample Site Background

This research focuses on marine sediments and pore waters collected from the Costa Rica margin during IODP Expedition 344. IODP Expedition 344 set sail on the JOIDES Resolution in October 2012 with the goal of studying the convergent margin off the west coast of Costa Rica (Expedition 344 Scientists, 2013b). This margin features the subduction of the oceanic Cocos Plate under the Caribbean Plate

near the Osa Peninsula (see Figure 2). The age of the subducting seafloor is ~15 Ma (Barckhausen et al., 2001), which is subducting at a rate of around 90mm/y (DeMets, 2001). The tectonic activity of the Costa Rica margin has been linked to the transfer of fluids through the sediments in previous research (Shipley et al., 1990; Kahn et al, 1996; Ruppel and Kinoshita, 2000; Silver et al., 2000; Hensen and Wallmann, 2005). Evidence for fluid flow includes increased methane in deep sediments along the margin (Ruppel and Kinoshita, 2000), colonies of chemosynthetic organisms present at seafloor that are consistent with those found near seafloor vents (Bohrmann et al., 2002), and the presence of mud volcanoes that resulted from fluid migration along the accretionary wedge in the Costa Rica margin (Shipley et al., 1990). The fluids moving through this region are thought to be expelled at the highest rate near the trench (Shipley et al., 1990). The source of the fluid moving through the sediments of the Costa Rica margin is most likely from both sediment compaction, moving some fluids upward, and from deep faults trending parallel to the trench along the subducting Cocos plate (Silver et al. 2000). The temperature of the transported fluid along the margin and the chemical composition suggest the fluids are sourced from deep subducted sediment and are not entirely unmodified, with a composition of about half seawater and half subduction fluids sourced from the forearc basin (area between volcanic arc and the ocean trench) (Fuller et al., 2005; Hensen and Wallmann 2005; Solomon et al., 2009).

Expedition 344 Scientists determined the ages and sedimentation rates at the various drill sites. Ages of lithologic units were constrained via identification of

microfossils present within the sediments. Sedimentation rates were interpreted from biomagneto-stratigraphic data (Expedition 344 Scientists, 2013a). Unit I of Hole U1381C was dated as early Pleistocene (~1-2Ma); Unit II yielded an age of 11-13 Ma (Miocene). The average rate of sedimentation at the site was determined to be 80-110 meters per million years (m/my). Hole U1413B Unit I was dated as early Pleistocene. More refined dating was not possible because the radiolarians present were poorly preserved (Expedition 344 Scientists, 2013a). The average rate of sediment accumulation at Hole U1413B was found to be 221m/my. Units I, II, and III of Hole U1414A were dated as Holocene, mid-to-late Pleistocene, and early Pleistocene, respectively. Unit I of Hole U1414A was found to have an average sedimentation rate of 590 m/my, while the lower two units yielded an average rate of 383 m/my. Any units without specific dates in this discussion lacked adequately preserved microfossils (Expedition 344 Scientists, 2013a). Hole U1414A is on the subducting plate and is the site closest to the trench. Hole U1381C is on the subducting plate ~10 km from the trench, and Hole U1314B is ~30 km from the trench and is located on the Caribbean plate (Expedition 344 Scientists, 2013a). Given the seismic activity in this region, the Costa Rica margin holds potential for discovery of unique biogeochemical signals and controls. The goal of this research is to explore the biogeochemistry of the dynamic Costa Rica margin through a study of stable sulfur isotopes combined with measurements of sulfur compounds, iron speciation, and application of Rayleigh Distillation models to assess isotopic fractionation within these systems.

2. Materials and methods

2.1 Sample Collection and Preservation

Samples were taken from Integrated Ocean Drilling Program (IODP) Expedition 344 in the Costa Rica margin from Holes U1414A, U1413B, and U1381C at water depths of 2458.6m, 540.4m, and 2064.6m, respectively (see Table 1 for more details on site location and depth). This study uses both the pore waters and the marine sediments collected during throughout the duration of the expedition. Expedition 344 Scientists extracted the pore waters analyzed in this research while on board the JOIDES Resolution within 24 hours of initial core recovery (Expedition 344 Scientists, 2013). Sediments from the cores were first pared down to remove portions that may have been oxidized or contaminated with seawater. After prepping the sediment cores, segments were cut and squeezed to expel pore water following method and instrument design described in Manheim and Sayles (1974)

Core	Latitude	Longitude	Sample Depth Range (mbsf)	Location Relative to subduction Trench
1381C	8°25.7027′N	84°9.4800′W	0-105m	On subducting Cocos plate, about 10km away
1413B	8°44.4593′N	84°6.7992′W	0-30m	On Caribbean plate, about 30km from trench
1414A	8°30.2304′N	84°13.5298′W	0-350m	On subducting Cocos plate, core nearest trench (<10km away)

Table 1. Core location and depth.
IODP Expedition 344 scientists collected sediments from seven primary sites each with multiple drill holes. Included is information only on the three holes and sample depths this research focuses on. Depth ranges begin with zero representing sea floor. Water depth at these sites ranges from 540.4-2064.6 meters (Expedition 344 Scientists, 2013a).

(Expedition 344 Scientists, 2013b). For a detailed table of samples used and depth intervals of each, see Appendix.

2.2 Sequential Iron Extraction

To quantify iron oxides within the sediments, sequential iron extractions were conducted. Unless otherwise indicated, all extractions were performed using 200 mg of frozen sediment in 15 mL centrifuge tubes with 10 mL of solution. Because these samples are modern marine sediments, they were stored frozen to minimize oxidation, and all solutions were degassed with nitrogen for 30 minutes. For iron extraction, a 1 M sodium acetate solution with a pH of 4.5 was prepared by dissolving sodium acetate in DI water, adjusting the pH to 4.5 with glacial acetic acid. 10 mL of the degassed sodium acetate was added to 200 mg of frozen marine sediment in a 15 mL centrifuge tube and placed on a shaker table for 24 hours at room temperature to remove the carbonated associated iron such as siderite and ankerite (modified method from Poulton and Canfield, 2005; Ferdelman, 1988). At the end of the timed extraction, the 15mL centrifuge tubes were spun for 3 minutes at 5000 rpm in a centrifuge, the supernatant was decanted into a 2 mL Nalgene vial, excess supernatant was discarded, and the sediment remained in the tube for the next solution in the sequential extraction procedure.

An ascorbic acid solution prepared with DI water, ascorbic acid, and sodium bicarbonate and adjusted to a pH of 7.5 was added in the amount of 10 mL per sample (Raiswell et al., 1994). The components were contained in 15 mL centrifuge

tubes, placed on a shaker table, and left to agitate for 24 hours at room temperature to extract adsorbed Fe, ferrihydrite, and amorphous iron phases. A sodium dithionite solution was prepared by combining DI water, sodium citrate, and sodium dithionite and adjusted with acetic acid to pH 4.8. A 10 mL aliquot of this sodium dithionite solution was added to the sediment sample and shaken on a shaker table for 2 hours at room temperature to extract goethite, akagenéite (an iron oxide-hydroxide which forms from weathering of pyrrhotite) (Refait and Génin, 1997) and hematite.

A pH 3.2 ammonium oxalate solution was prepared using DI water, oxalic acid, and ammonium oxalate; 10 mL were added to each sample tube. The tubes were placed on a shaker table at room temperate for 6 hours to remove magnetite. At the termination of each of the above extraction steps, the resultant solutions were decanted into 8 mL containers for later analysis of Fe abundance using an Agilent 7400 ICPMS. Also, acid-soluble iron phases were extracted from dried, homogenized sediment using the standard degree-of-pyritization method (Raiswell et al., 1988): boiling concentrated HCl in a glass test tube held over an open flame for 1 minute to heat the sample and an additional 1-minute period with the acid boiling. After the 1-minute period of boiling, the reaction was quenched with DI water and volumetrically diluted (Raiswell et al., 1994). After centrifugation, the supernatant was treated with Ferrozine was analyzed for iron content via colorimetry (Viollier et al., 2000).

2.3 Sulfur Analysis

Except for the sulfate concentration measurements, which were determined onboard the expedition vessel by Expedition 344 Scientists using a Metrom 861.004 Advanced Compact ion chromatograph (Expedition 344 Scientists, 2013b), all other sulfur analysis steps were carried out in the biogeochemistry lab at the University of California, Riverside. Pore water sulfides were assessed using a spectrophotometer by adding methylene blue to DI-water-diluted samples, allowing color to develop in capped tubes in the dark for 20 minutes, followed by colorimetric measurement at a wavelength of 670 nm (Cline, 1969). Elemental sulfur was extracted by adding 25 mL of degassed methanol to 2 g of frozen sediment in a 50 mL centrifuge tube, mixed via vortex, and placed on a shaker table to agitate the samples for 24 hours. The resultant extract was then decanted and sent to a third party for analysis via high performance liquid chromatography (HPLC) to assess abundances of elemental sulfur (Li et al., 2008). Using the sediments left over from elemental sulfur extraction, the samples were transferred to a glass vessel for further sulfur speciation using the N_2-flushed apparatus setup outlined by Canfield et al. (1986).

Acid-volatile sulfide (AVS) was extracted using 6M HCl for 1 hour, while allowing the distilled precipitate to collect in 15 mL centrifuge tubes filled with a freshly prepared zinc acetate solution (Allen et al., 1993). The AVS extraction was performed at room temperature, often described as a 'cold extraction,' to remove mackinawite, greigite, and amorphous monosulfides. This method was chosen over

a hot extraction because it should yield full dissolution of the desired compounds in these modern marine sediments (Cornwell and Morse, 1987). In contrast, a hot extraction is typically used for samples that are expected to contain high levels of pyrrhotite or large crystalline mackinawite particles (Cornwell and Morse, 1987; Rickard and Morse, 2005). Upon completion of the AVS step, the zinc acetate tubes were removed from the apparatus, capped, and set aside for later analysis. Next, 25 mL centrifuge tubes of fresh zinc acetate were placed on the apparatus to collect the precipitate from the chromium-reducible sulfur distillation procedure (CRS) for determination of pyrite immediately following the AVS step. Sediment in the glass vessels remained in place while a solution of 12M HCl and 1M chromic chloride was added via syringe to the samples (in addition to the 6M HCl solution left in the reaction vessel from the AVS step) and allowed to react for 2 hours (Canfield et al., 1986). Throughout the entire 2-hour reaction, the vessels were heated via hotplate to 250°C to maximize digestion (Gröger et al., 2009). Sulfide concentrations were measured using the methylene blue method (Cline, 1969) and the zinc sulfide collected in AVS and CRS distillation traps (Canfield et al., 1986). The remaining zinc sulfide was transformed to silver sulfide by adding silver nitrate to solution—allowing the precipitate to form spontaneously. The resulting Ag_2S was filtered, dried, and homogenized before isotopic analysis using a Thermo-Scientific Delta V Isotope Ratio Mass Spectrometer (IRMS). The protocol to determine total organic sulfur (TOS) within the samples is based on high temperature combustion of dried homogenized sediment in an ELTRA furnace (see Section 2.5).

2.4 Sulfur Isotopes

Pore waters collected and preserved with zinc acetate during IODP Expedition 344 were used to analyze sulfur isotope fractionation within the Costa Rica margin sediments. Pore water tubes were centrifuged to isolate the precipitate. Supernatant from the centrifuged pore water was then decanted into glass test tubes, to which a freshly prepared and filtered barium chloride solution was added in the amount of 2 mL per each 5 mL of supernatant. After covering with Parafilm, the tubes were left at room temperature for 72 hours to allow for full transformation to barium sulfate. The newly formed compound was then filtered from the solution, dried, homogenized, and set aside for analysis by IRMS. Zinc sulfide from pore waters collected after centrifugation was reacted with silver nitrate solution. The resulting silver sulfide was then filtered using Millipore nitrocellulose filters. After allowing the filtered Ag_2S to dry, it was homogenized, weighed into tin capsules along with vanadium pentoxide, and then combusted in a Thermo-Scientific Delta IRMS.

2.5 Total Organic Sulfur, Total Organic Carbon, Total Inorganic Carbon

Total organic sulfur (TOS) was measured by combusting rinsed and dried residues remaining from the CRS/AVS steps using an ELTRA furnace and ELTRA Carbon/Sulfur Determinator. Total organic carbon (TOC) and total inorganic carbon (TIC) were both measured onshore by IODP Expedition 344 Scientists following the sampling cruise (Expedition 344 Scientists, 2013a).

2.6 Rayleigh Distillation Model

An Excel spreadsheet was created based on Equation 4, where ƒ is the sulfate concentration at depth divided by the original concentration in overlying seawater. To calculate the fractionation factor required to create the end sulfate isotope ratios of interest, the equation requires inputting the beginning isotope ratio of the sulfate pool (such as the seawater average $\delta^{34}S\text{-}SO_4$ of 20‰), a fractionation factor and the concentration ratio between the original and remaining sulfate pools. With these values entered into the model, each variation of epsilon (representing the fractionation factor) changes the output for $\delta^{34}S\text{-}SO_4$ for when there is no sulfate remaining ($\delta^{34}S_t$). The number input for epsilon was adjusted until the $\delta^{34}S_t$ was equal to or near that of the heaviest $\delta^{34}S\text{-}SO_4$ measurements in each core modeled thereby indicating the fractionation factor required to create the values found in this study.

3. Results

3.1 Pore water Data

3.1.1 Sulfate, sulfide, and methane concentrations

Pore water sulfate from Hole U1381C shows variation down the sediment column; with 26.7 mM at the top sample around 1.6 mbsf, 12 to 20 mM mid-depth (14-85 mbsf), and 22-25mM in the bottom 20 meters of the sampled sediments. Methane concentrations at Hole U1381C are low, with an average of 4 ppmv throughout the sediment column. In the bottom sediments (between 84 an 103

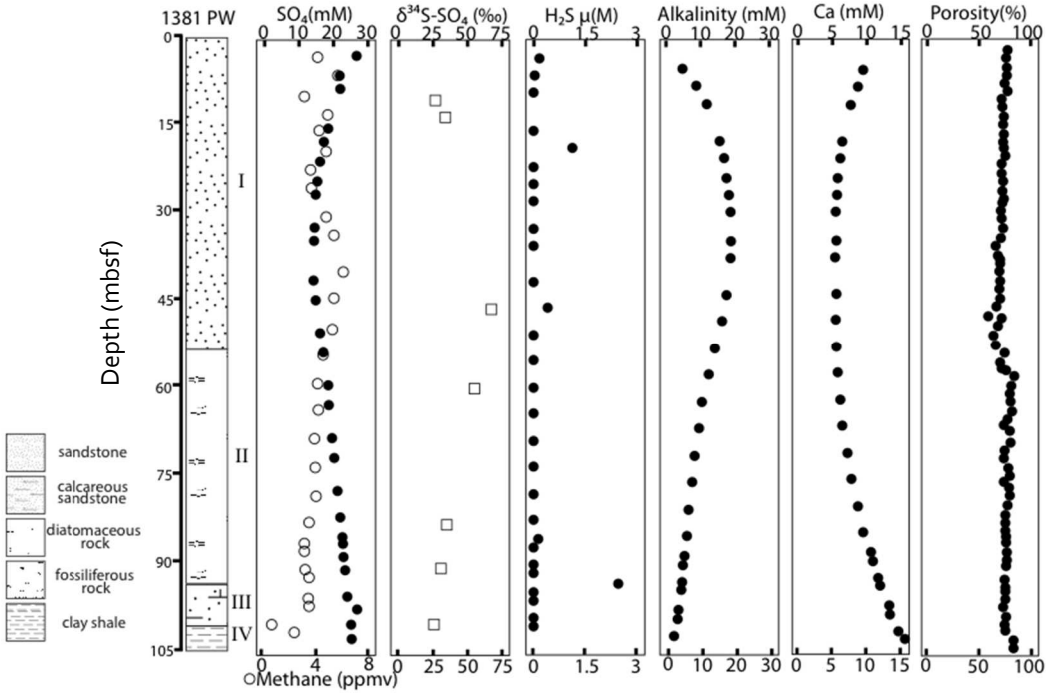

Fig 3. Lithology and pore water profiles for Hole U1381C. Pore water sulfate (SO4; filled circles), methane (open circles), alkalinity, and calcium (Ca), as well as porosity were measured on board the JOIDES Resolution during IODP Expedition 344 (Expedition 344 Scientists, 2013b). Data for pore water sulfate isotope ratios ($\delta^{34}S\text{-}SO_4$) and sulfide concentrations (H_2S) were measured at University of California, Riverside for this study. Roman numerals refer to their corresponding lithologic units discussed in the text. For ages of units, see section 1.5.

mbsf) of Hole U1381C, pore water methane drops to between 2 and 4 ppmv. Hole U1413B shows 25 mM of sulfate in pore water, which stays level until a sharp drop to zero at the sulfate-methane transition (SMT) at ~17 mbsf. Methane measured in headspace gas samples from Hole U1413B is present in trace amounts (2-10 ppmv) in the upper 10 meters (Expedition 344 Scientists, 2013b). Approaching the SMT, the methane in Hole 1413B raises rapidly to 30, 119, 364, and then 13,000 ppmv. Methane values in Hole 1413B remain between 13,000-17,000 ppmv from the SMT around 15 meters to the cores bottom of the pore waters from the hole, except for

one data point of 42,600 ppmv at 24 mbsf. This well-defined SMT can be seen clearly in Figure 3.

Hole U1414A has a unique sulfate profile featuring two dips and a sort of plateau in concentration across a long span of depth between the two minimums. The top sample from the sediments at 0.55 mbsf has a sulfate concentration of 27.6 mM and sulfate concentration between 90 and about 280 mbsf in Hole 1414A is relatively constant with values between 14.2 and 16 mM (averaging ~15 mM) The

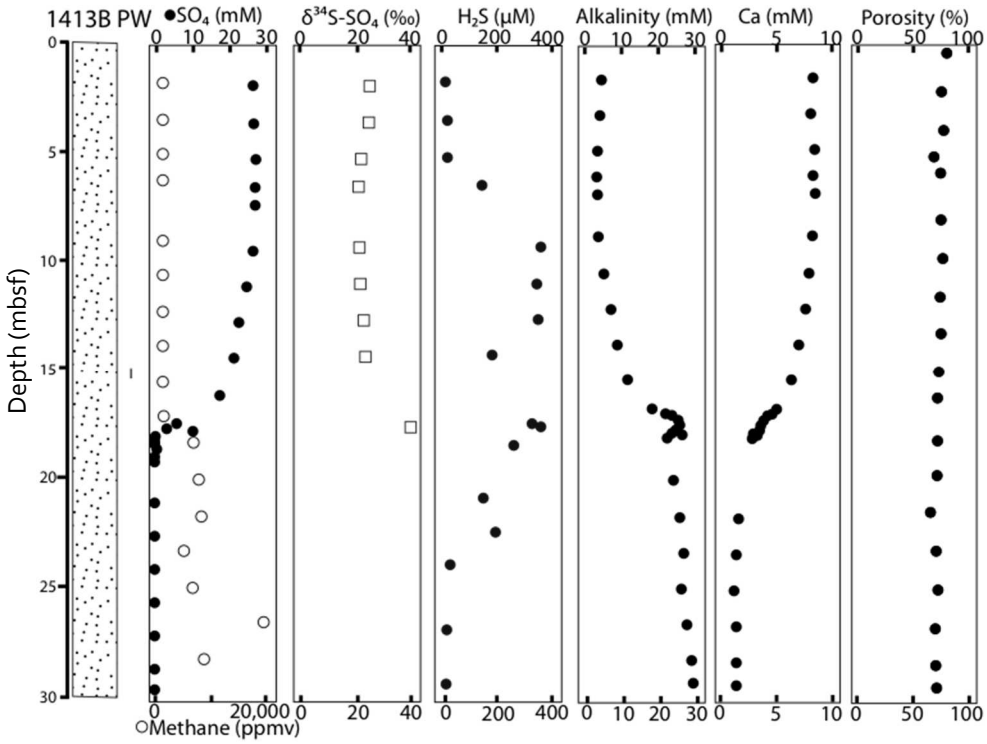

Fig 4. Pore water profiles for Hole U1413B. SO_4 indicates sulfate measured onboard the JOIDES Resolution by IODP Expedition 344 Scientists. Methane, alkalinity, calcium (Ca), and porosity were also measured during the expedition. Data for pore water sulfate isotope ratios ($\delta^{34}S$-SO_4) and sulfide concentrations (H_2S) were measured at University of California, Riverside. For lithological details, see Figure 3.

first dip in the sulfate concentration profile from Hole U1414A ranges 4-5 mM, while the lower drop near the bottom drops to 2 mM SO_4. The upper minimum is around 45 mbsf, while the lower is at 315 mbsf. Between 315 mbsf and the bottom samples of the sediments from Hole U1414A, sulfate increases again, rising from the minimum of 2 mM up to 12 mM. Methane at this hole is low (<10 ppmv) from 0 to 180 mbsf. Below 180 mbsf, methane ranges from 15-40 ppmv.

Holes U1381C and U1414A both have very low H_2S (<3.5 μM) throughout.

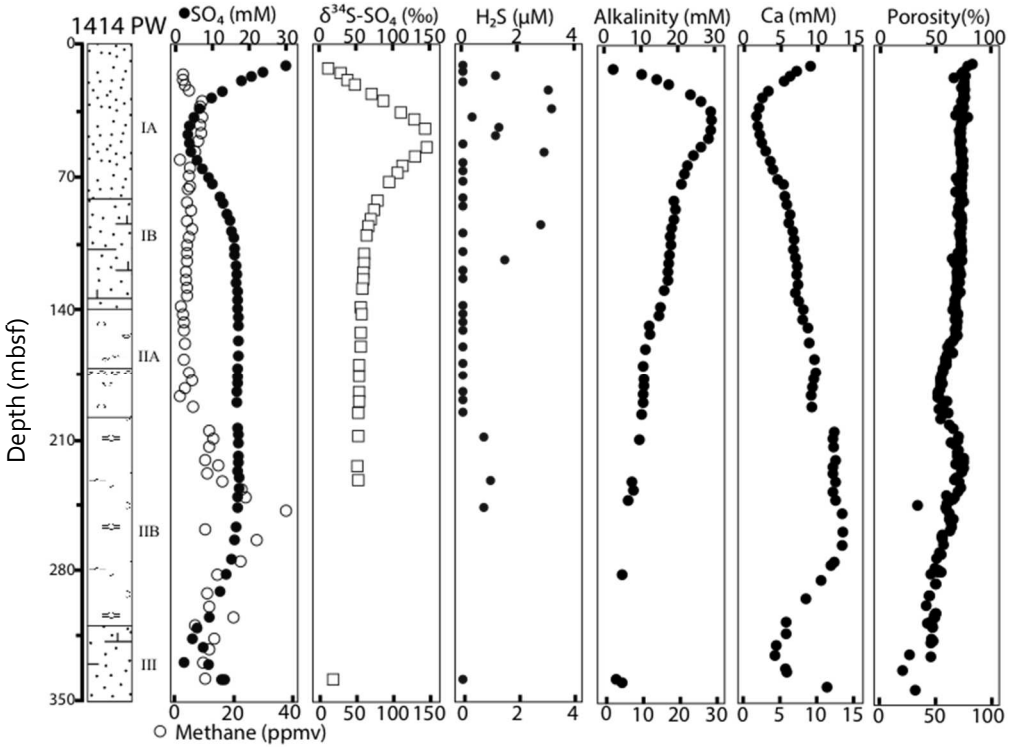

Fig 5. Pore water profiles for Hole U1414A. SO_4 indicates sulfate measured onboard the JOIDES Resolution by IODP Expedition 344 Scientists. Methane, alkalinity, calcium (Ca), and porosity were also measured during the expedition (Expedition 344 Scientists, 2013b). Data for pore water sulfate isotope ratios ($\delta^{34}S$-SO_4) and sulfide concentrations (H_2S) were measured at University of California, Riverside. Gaps in $\delta^{34}S$-SO_4 and H_2S are due to lack of available samples for the corresponding depths. For lithological details, see Figure 3.

Pore water sulfide in Hole U1413B ranged from around 10 μM at the top and bottom of the sediments to around 350 μM between 7 and 16 mbsf.

3.1.2 Sulfate isotopes

In Hole U1381C, the sulfate isotope signature ($\delta^{34}S\text{-}SO_4$) ranges from +25-75‰, with the peak near 45 mbsf. Below the depth where $\delta^{34}S\text{-}SO_4$ values are heaviest, the sulfate isotope ratios gradually become lighter down the sediment column with the bottommost pore waters having a $\delta^{34}S\text{-}SO_4$ of +25‰. The $\delta^{34}S\text{-}SO_4$ in Hole U1413B is nearly constant down the sediment column at around 25‰. The bottom sample from Hole U1413B near 27 mbsf had a measured $\delta^{34}S\text{-}SO_4$ about +40‰. In Hole U1414A, the sulfate isotope profile begins at 0.55 mbsf with a $\delta^{34}S\text{-}SO_4$ of +24‰ and peaks around 45 mbsf at +141‰. The $\delta^{34}S\text{-}SO_4$ at this site then drops down core, reaching +70‰ near 85 mbsf, and remains steady for about 190 m. The bottom-most pore water sample from Hole U1414A at the depth of 320 mbsf had a measured $\delta^{34}S\text{-}SO_4$ of +29‰.

3.1.3 Alkalinity and Calcium Concentrations

At all three analyzed sites pore water alkalinity and calcium contents vary inversely. In Hole U1381C, alkalinity begins with a concentration of 4.4 mM with a calcium concentration of 10 mM in the top sample from the core, at 1.5 mbsf. As alkalinity rises to the peak of about 20 mM near 30 mbsf, calcium varies inversely, dropping to about 5 mM. In Hole U1381C, calcium reaches 15 mM at a depth of 105

mbsf as alkalinity drops again, reaching as low as 3 mM. In Hole U1413B, calcium starts at around 8 mM at the top sample from the core (1.4 mbsf), while alkalinity is at 5 mM. Alkalinity values rise to 30 mM at a depth of about 18 mbsf, calcium drops to about 2 mM. Both alkalinity and calcium values are constant from 18 mbsf until the bottom of the core at 30 mbsf. Hole U1414A shows a sharp drop in calcium from 10 mM to 4mM between the top of the core at 0.55 mbsf and the minimum of the calcium profile at 28 mbsf. Corresponding to this curve, the alkalinity in Hole U1414A begins 4.45 mM in the top sample from the hole (0.55 mbsf) and reaches nearly 32 mM around 28 mbsf. Between 45 and 275 mbsf, calcium steadily rises to about 13 mM—again corresponding to a mirrored curve in the alkalinity, which drops 6mM between 270 and 330 mbsf. Between 270 and 330 mbsf, calcium dips to 3 mM and again increases, reaching a concentration of 12 mM in the bottom samples from the hole.

3.1.4 Porosity

Measurements of porosity in Hole U1381C range from 75-79% in the upper 30 meters, 66-73% between 30-50m, and 75-82% in the bottom half of the hole (50-103 mbsf). Hole U1413B porosity is 66-72% in the upper 13 meters and ranges from 63 to 65% between 15 and 26 mbsf. In Hole 1414A, from the top of the hole to a depth of about 30 mbsf, porosity ranges from 75 to 82% and from 65 to 74% between 30 and 175 mbsf. Between 175 mbsf and 210 mbsf, porosity drops to 50-

65%. From 210 mbsf to the bottom of the hole (at 310 mbsf), the porosity drops from 50% to around 25%.

3.2 Solid Phase Data

3.2.1 Total Organic Carbon

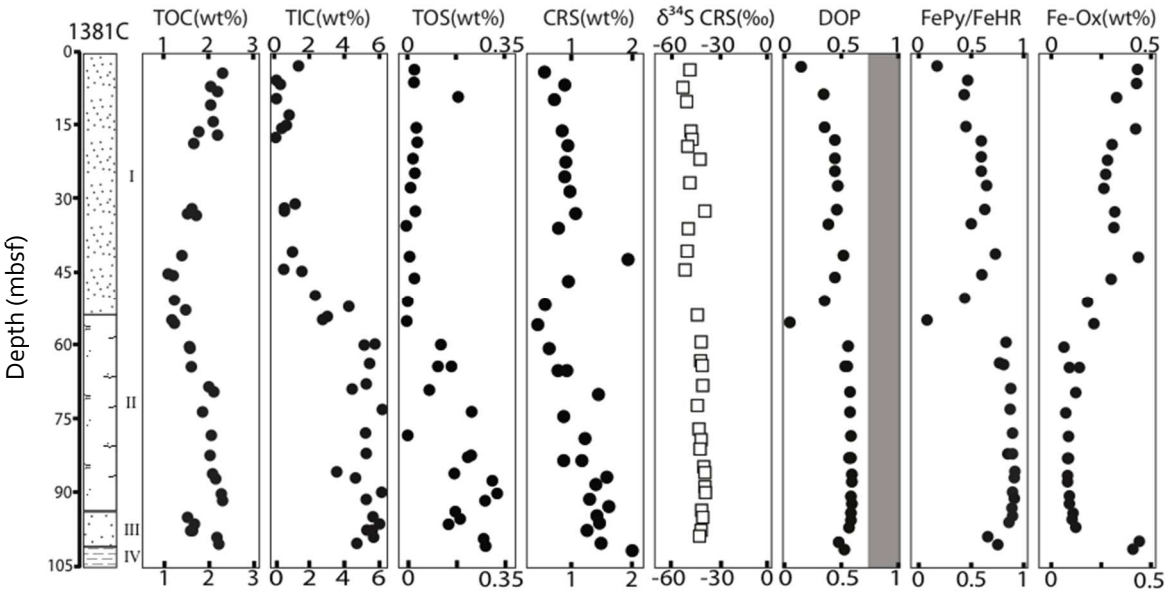

Fig 6. Solid phase chemical profiles for Hole U1381C. TOC=total organic carbon, TIC=total inorganic carbon. Both TOC and TIC data sets are from IODP Expedition 344 Scientists (Expedition 344 Scientists, 2013b). TOS= total organic sulfur. CRS= chromium reducible sulfur (pyrite and FeS). δ^{34}S-CRS represents sulfur isotope ratios of CRS precipitate. DOP= degree of pyritization calculated as pyrite iron/(pyrite iron + reactive iron). The gray bar on the DOP graph indicates values associated with anoxic deposition (Raiswell and Berner, 1985). Fe_{Py}/Fe_{HR}= ratio of pyrite iron/(pyrite iron + total iron oxides) but does not include AVS (acid volatile sulfur) because it was below detection. Fe-Ox= total iron oxides, sum of products ascorbic acid, sodium dithionite and ammonium oxalate steps of Fe extraction. For lithological details, see Figure 3.

Sediments from all three holes analyzed have TOC less than 3 wt%. In Hole U1381C, TOC values average 2 wt%, and in Hole U1413B, TOC values range from 1.85 wt% at the top of the core and as low as 1.16 wt% at the bottom of the sampled

core interval. Hole U1414A has 2 wt% at the top of the core, an average of 1.5 wt% between 70 mbsf and 300 mbsf, and a cluster of samples with measured TOC of 1.5-2.5 wt% between 315 and 350 mbsf.

3.2.2 Total Inorganic Carbon

In Hole U1381C, measured TIC is <2 wt% in the upper half of the sampled sediments, while the bottom half of the averages 5 wt%. In Hole U1413B, TIC is around 1.5 wt% throughout the length of the core. In Hole U1414A, TIC is ~1.5 wt% from 0-140 mbsf. The measured TIC values in Hole U1414A rise steadily to 8 wt%

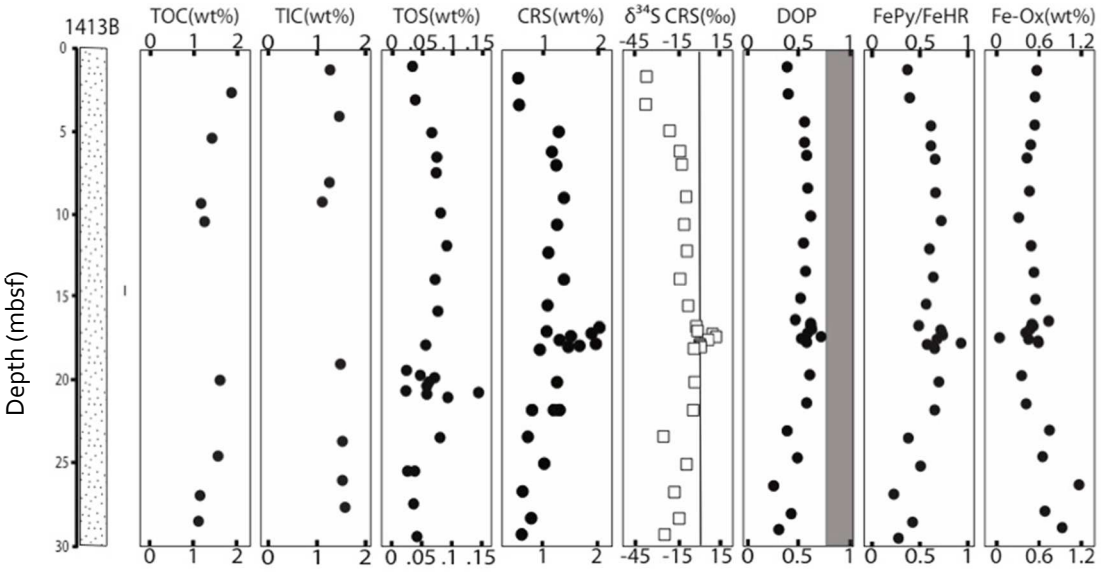

Fig 7. Solid phase chemical profiles for Hole U1413B. TOC=total organic carbon, TIC=total inorganic carbon. Both TOC and TIC data sets are from IODP Expedition 344 Scientists (Expedition 344 Scientists, 2013b). TOS= total organic sulfur. CRS= chromium reducible sulfur (pyrite and FeS). δ^{34}S-CRS represents sulfur isotope ratios of CRS precipitate. DOP= degree of pyritization calculated as pyrite iron/(pyrite iron + reactive iron). The gray bar on the DOP graph indicates values associated with anoxic deposition (Raiswell and Berner, 1985). Fe_{Py}/Fe_{HR}= ratio of pyrite iron/(pyrite iron + total iron oxides). Fe-Ox= total iron oxides, sum of products ascorbic acid, sodium dithionite and ammonium oxalate steps of Fe extraction. For lithological details, see Figure 3.

between 140 and 210 mbsf and drop to 5 wt% near 245 mbsf and then rise back up to 8 wt% toward the bottom of the hole.

3.2.3 Total Organic Sulfur

The TOS in Hole U1381C is around zero from the top of the sediment column down to about 60 mbsf, where TOS measurements span from 0.1-0.3 wt% between 60 and 100 mbsf. In Holes U1413B and U1414A, average TOS measurements are around 0.05 wt%.

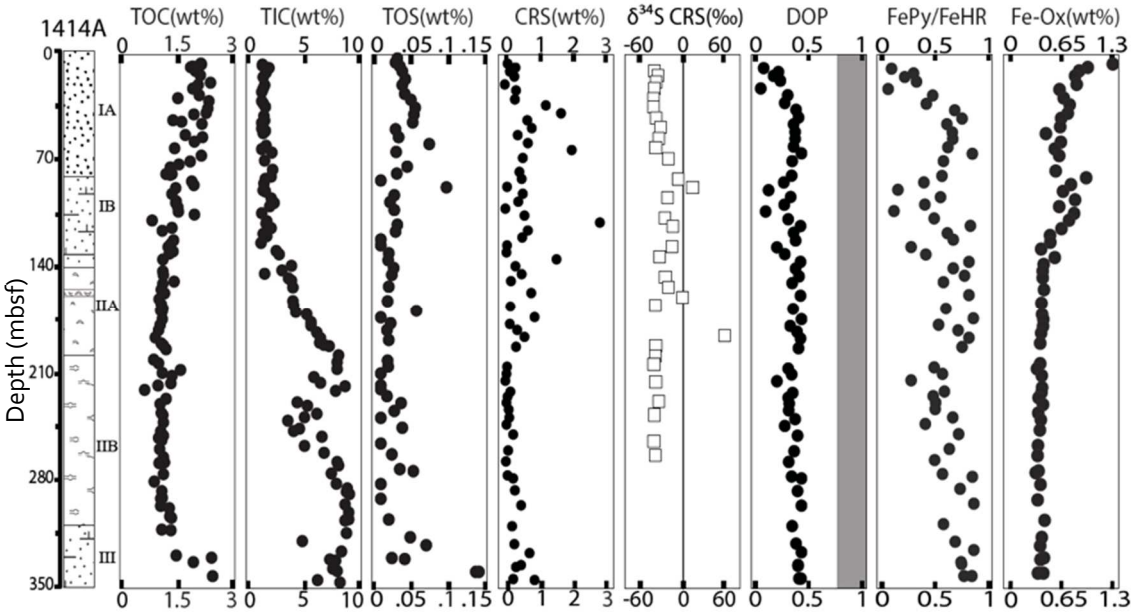

Fig 8. Solid phase chemical profiles for Hole U1414A. TOC=total organic carbon, TIC=total inorganic carbon. Both TOC and TIC data sets are from IODP Expedition 344 Scientists (Expedition 344 Scientists, 2013b). TOS= total organic sulfur. CRS= chromium reducible sulfur (pyrite and FeS). δ^{34}S-CRS represents sulfur isotope ratios of CRS precipitate. DOP= degree of pyritization calculated as pyrite iron/(pyrite iron + reactive iron). The gray bar on the DOP graph indicates values associated with anoxic deposition (Raiswell and Berner, 1985). Fe_{Py}/Fe_{HR}= ratio of pyrite iron/(pyrite iron + total iron oxides). Fe-Ox= total iron oxides, sum of products ascorbic acid, sodium dithionite and ammonium oxalate steps of Fe extraction. For lithological details, see Figure 3.

3.2.4 Chromium Reducible Sulfur and δ^{34}S-CRS

In all holes, the measurements of δ^{34}S-CRS increase as CRS abundance increases. In Hole U1381C, concentrations range from 0 to 2 wt%, while the measured values of δ^{34}S-CRS range between -50 to -45‰ throughout the length of sediment column. In Hole U1413B, CRS concentrations range from 0 to 2 wt%, with the highest values around 17 mbsf. The δ^{34}S-CRS in Hole U1413B is around -45‰ at the top of the hole, increasing to -10‰ between 5 and ~16.5 mbsf. Between 17 and 30 mbsf, δ^{34}S-CRS drops from around +10‰ to -30‰. The concentrations of CRS in Hole U1414A average 0.5 wt%, with higher values of 1-3 wt% scattered between 45 and 140 mbsf. The δ^{34}S-CRS in Hole U1414A averages between -55 and -30‰. Some samples have higher values, but only one at about 200 mbsf is significantly heavier—with a value of about +60‰.

3.2.5 Total Iron Oxides

In Hole U1381C, total iron oxides (the iron compounds removed in the ascorbic acid, sodium dithionite and ammonium oxalate steps of the sequential iron extraction protocol, see methods for more detail) range from 0.1-0.5 wt%, with a trend of decreasing values down the sediment column except for the two bottom-most samples each with 0.4 wt%. Holes U1413B has total iron oxides contents between 0.3 and 0.7 wt% in the upper 15 meters of the hole and a single data point of 0.1 wt% at 16 mbsf, before returning to the range of 0.3-0.7 wt %, which extends to a depth of 24 mbsf. The bottom three samples, between 24 and 26 mbsf, have

higher values, with a range of total iron oxide contents of 0.7-1.1 wt%. In Hole U1414A, the highest measured values are present in the top 16 meters of the hole, with values of 0.7-1.3 wt%. Between 18 and 70 mbsf, total iron oxide contents are 0.2-0.6 wt% and 0.4-0.9 wt% from 70 to 110 mbsf. Values in the bottom 200 meters of Hole U1414A range between 0.1-0.4 wt %, averaging 0.1 wt%.

3.2.6 Degree of Pyritization and Ratio of Pyrite Iron to Highly Reactive Iron

Degree of pyritization values for all cores are between 0 and 0.5—values consistent with deposition in an oxic marine environment (Canfield and Raiswell, 1985). Ratios of pyrite Fe over highly reactive were used rather than the common calculation of [(pyrite +AVS)/highly reactive iron] because AVS was below detection in all samples. Fe_{Py}/Fe_{HR} in Hole U1381C and Hole U1414A both show values ranging from 0 to nearly 1, with the highest values in the lower portions of the sediment columns. For Hole U1413B, Fe_{Py}/Fe_{HR} values average under 0.5, with a brief increase to about 0.8 around 17 mbsf.

3.2.7 Rayleigh Model Output

Rayleigh model calculations for three different fractionation factors were considered for the two sites that showed heavy pore water sulfate $\delta^{34}S\text{-}SO_4$ values. Two different input values were considered: the modern seawater average $\delta^{34}S\text{-}SO_4$ of +20‰, and the heavy sulfate isotope ratio (+65-70‰) seen for 190 meters below the maximum $\delta^{34}S\text{-}SO_4$ value—the latter was included to explore the

possibility of upward fluid flow within the sediments. After calculating the output for fractionation factors (see Table 2) and the two possible $\delta^{34}S\text{-}SO_4$ inputs, the epsilon range of -50 to -55 best fit the plotted data for Hole U1414A if the input source has the value of the modern seawater average for $\delta^{34}S\text{-}SO_4$ (+20‰) (see Figure 8). An epsilon value of -45 to -50 best fits the data from Hole U1414A, if the isotope ratio of the initial sulfate pool was that of the heavy sulfate pool (using $\delta^{34}S\text{-}SO_4$ =+65‰) between 90 and 280 mbsf. For Hole U1381C, a fractionation factor of -25 best fits data when the initial isotope ratio of the sulfate pool is equal to that of seawater (+20‰).

Hole	δ initial ‰	ε	δ end ‰
U1414A	20	-50	135
U1414A	20	-55	146
U1414A	65	-40	157
U1414A	65	-50	180
U1381C	20	-25	77
U1381C	20	-20	66

Table 2. Representative input and output values for Rayleigh Model. To model differing scenarios, isotope values for the input source were varied as shown. 'δ initial' corresponds to the isotope ratio in either average seawater or that measured in the portion of the hole listed as the input source in the first column. 'δ end' represents the isotope ratio measured in pore water samples. ε=(α-1)*1000 (see methods for more detail).

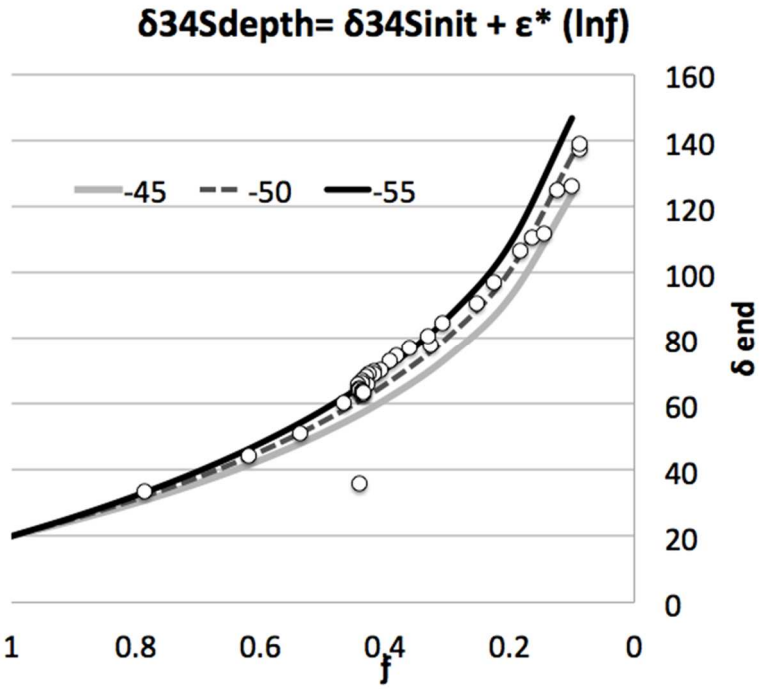

Fig 9. Rayleigh model output fit with Hole U1414A data. Data and model output created using the equation: $\delta^{34}S_{depth} = \delta^{34}S_{init} + \varepsilon^* (\ln f)$ f=(end SO_4 concentration/initial concentration). Values correspond to epsilon (fractionation factors), ε=(α-1)*1000 (see methods for more detail). δ end represents the isotope ratio measured in pore water samples. Open circles are plotted data from Hole U1414A

4. Discussion

4.1 Chemical profiles implications of biogeochemical cycling

The presence of both sulfate and methane throughout the length of both Hole U1381C and Hole U1414A may indicate that sulfate reducing microbes and methanogens are both present throughout the sediment column or it is possible that methane is diffusing into the sulfate-rich portion of the sediments. There have been reports of sulfate reducing prokaryotes existing alongside methanogens and methane–oxidizers (Hoehler et al., 1994; Jørgensen and Nelson, 2004; Knab et al.,

2008; Holmkvist et al., 2011). These relationships may be relevant, for example, in communities of mixed metabolisms in which methane oxidizers near methane seeps appear to facilitate greater sulfate reduction (Iversen and Jørgensen, 1985; Hoehler et al., 1994; Jaye et al 2004). Hole U1414A not only lacks a distinct SMT but also shows no distinct relationship between the two compounds, likely because methane is present in such low concentrations (<4 μM throughout the entire length of the sediment column). The methane levels increase in the pore waters below 220 mbsf but decrease again, possibly indicating an increase of microbial methanogenesis in the sediments at those depths. The maximum methane in the pore waters in Hole U1414A, however, is relatively low (<40 ppmv) compared to the much higher values seen below the SMT in Hole U1413B. At two levels within the sampled pore waters, Hole U1414A exhibits sulfate decreases (from 30 to 15 mM between 0 and 40 mbsf) consistent with microbial sulfate reduction. Sulfate rising at depth, however, is not consistent with any known process in a steady-state setting. A similar relationship was noted by Böttcher et al. (2004), where pore water sulfate increased from 15 to 25 mM at a depth of 200 mbsf in the sediments from the Campbell Plateau—a site in the South Pacific with microbial sulfate reduction rates similar to those found at the Cascadia Margin, a site tectonic similarities to the Costa Rica margin and has further relevance noted below (Rudnicki et al., 2001). The sulfate in Hole U1414A is never fully depleted, suggesting there is a continual sulfate source that prevents complete removal via microbial sulfate reduction. The source is not likely to be dissolution of

barite because the local sulfate concentrations are too high to allow for undersaturation (Breymann et al., 1992; Torres et al., 1996; Riedinger et al., 2006).

It is important to highlight the wide variation of methane concentrations among the three sample sites. Methane is commonly found to be abundant along continental margins (Shipley et al., 1979; Ritger et al., 1987; Kvenvolden, 1988). More specifically, past research in the study area of the Costa Rica margin has revealed upward flow related to the formation of methane hydrates (Hensen and Wallmann, 2005). The three sites used in this study are located near the western boundary of the Caribbean plate, and the only site on this plate, Hole U1413B, features abundant methane. On the Cocos plate, Hole U1381C and Hole U1414A feature averages of less than 8 and 40 ppmv of methane, respectively. This pattern may be due to the relatively lower levels of methanogenesis within those sediments corresponding with the observed lack of reactive organic matter (TOC is 0.7-2.2 wt% in Hole U1414A) and/or because of microbial consumption of methane.

With the trends of sulfate concentration observed among the three holes, we can expect to find corresponding patterns in the concentrations of sulfide (Berner, 1989). Hole 1413B illustrates such a relationship with hydrogen sulfide increasing at the depths where sulfate is seen to be decreasing. Holes U1381C and U1414A both have levels of sulfide that are at or only slightly above zero levels over the full range of sampled depths. This lack of sulfide could be explained if the region had sufficiently high detrital sedimentation rates such that delivery of highly reactive iron kept pace with rates of sulfide production. At the same time, however, high

rates of sediment burial have been linked to increased rates of microbial sulfate reduction and rapid depletion of dissolved sulfate (Berner, 1978; Canfield and Berner, 1987).

In all three of the sampled sites (Figures 6, 7, and 8), alkalinity and TOC show a relationship that is consistent with decomposition organic matter (decreasing TOC abundance) during microbial sulfate reduction which increases dissolved inorganic carbon (DIC) and drives up alkalinity concentrations (Abd-el-Malek and Rizk, 1963; Berner et al., 1970). When observing the relationship between calcium concentrations and alkalinity in Holes U1381C, U1413B, and U1414A, one can see that there is an inverse relationship between the two (Figures 3, 4, and 5). The calcium profile in Hole U1414A features a sharp drop corresponding to the decrease of alkalinity around 330 mbsf where there may be precipitation of carbonates (Garrels and Christ, 1965). At the SMT in Hole U1413A, alkalinity is increasing and calcium is decreasing, likely reflecting precipitation of calcium carbonate as a consequence of anaerobic oxidation of methane and associated production of alkalinity (Luff and Wallmann, 2003).

In studies of other continental margins, there has been evidence reported for tectonically driven fluid advection (e.g. Torres et al, 1996). More specifically, movement of fluids deep within sediments at the Costa Rica margin has been observed to be occurring diffusely and in some cases focused along fractures (Kahn et al., 1996; Ruppel and Kinoshita, 2000; Hensen and Wallmann, 2005). Results from IODP Expedition 344 suggest fluid transport at sites of microbial methane oxidation

(Expedition 344 Scientists, 2013b). Fluid transport in the study region has been indicated by previous work, including release of fluid from the accretionary prism as reported by Kahn et al. (1996) and the upward movement of methane resulting in the formation of methane hydrates within Costa Rica Margin sediments (Hensen and Wallmann, 2005). Overall porosity trends at all three sites lend little insight into possible routes of fluid flow, since each shows a general trend of sediment compaction with increasing depth. However, more sporadic migration along the Costa Rica Margin through fractures or fissures is possible during compaction, as was suggested in Ruppel and Kinoshita (2000).

Degree of pyritization calculations for all three sites range from 0 to 0.5 (DOP maximum values are 1.0), which suggests sediment deposition under oxic conditions (Canfield and Raiswell, 1985). Values at the higher end of the observed range suggest effective pyritization of the detritally delivered Fe. Reactive iron is present in Holes U1413B and Hole 1414A at levels of ~1 wt%, even at depth, which suggests a long persistence of this biologically relevant substrate. The corresponding persistence of magnetite, as measured via the oxalate step of the sequential iron extraction protocol, may also reflect the general lack of hydrogen sulfide availability (Canfield and Berner, 1987). Reactive iron is known to buffer sulfide in marine pore waters, and therefore buildup of dissolved sulfide suggests iron limitation. Conversely, sulfide-limited regions would have iron remaining in the absence of dissolved sulfide (Canfield and Berner, 1987; Canfield 1989). In this light,

the depositional environments in Holes U1381C and U1414A are likely sulfide limited.

For Hole U1381C, the profiles of measured TOC indicate initial decreases in abundance as decomposition of organic matter couples to sulfate consumption in the upper 60 m of sediment. Between 60 and 100 mbsf, there is an increase of both TOC and TOS. Holes U1381C and U1414A also show nonsteady-state behavior, with a rise in TOC at depth (~330 mbsf). Such preferential preservation of organic matter is often linked to one of two conditions. One possibility is that the organic matter was deposited in abundance and preserved due to deposition under anoxic/euxinic settings (Canfield, 1989), but there are no indications in the iron chemistry or the sediment fabric for anoxic conditions. Alternatively, the sedimentation rate may have been higher, and bioturbation immediately following deposition was minimal—allowing for the preservation of compounds that would otherwise degrade in the presence of oxygen (Ingall and Van Cappellen, 1990; Canfield, 1994). The right balance must be struck, however, since greater sedimentation can also dilute the TOC content. Another consideration is the possibility that TOC remains because it is not readily reactive. Rather than being persevered, the organic matter may just be recalcitrant and thereby not able to be utilized during sulfate reduction (Canfield, 1993).

Hole U1414A TOC (See Figure 8) is lowest (0.5-1.1 wt%) in the interval of about 90-270 mbsf, where sulfate concentrations are around 15 mM, suggesting ongoing yet incomplete microbial reduction. The upper portion in Hole U1414A

contains simultaneously decreasing TOC and sulfate consistent with sulfate reduction (Westrich and Berner, 1984). Hole U1413B shows generally decreasing TOC abundance with depth as is often seen in marine sediments as a consequence of progressive microbial degradation (Jørgensen and Fenchel, 1974; Martens and Klump, 1984; Westrich and Berner, 1984).

In Holes U1414A and U1413B, TOS is low throughout most of both sediment columns at ~0.05 wt%, while in Hole U1381C, TOS ranges 0.1-0.3 wt%. The low organic sulfur contents likely reflect sulfurization of organic matter but under generally low pore water sulfide availability (Jørgensen, 1977; Werne et al., 2003).

4.2 Isotopic Signatures of Sites

Many of the observations of this study point to the occurrence of microbial sulfate reduction within the sediments of all three holes. The same can be said for the $\delta^{34}S\text{-}SO_4$ profiles. However, due to the uniquely heavy measurements in Hole U1381C and particularly Hole U1414A, the discussion of sulfate isotope ratios warrants special attention.

When comparing the $\delta^{34}S\text{-}SO_4$ measurements alongside the pore water sulfate concentrations for any of the three holes, one can see near-perfect mirror images of the profiles. Recall that as sulfate is depleted by way of microbial sulfate reduction, lighter isotopes are preferentially converted to sulfide while the remaining pore waters become correspondingly heavy (Goldhaber and Kaplan, 1974; Kendall and Caldwell, 1998). Thus, it is expected that as sulfate decreases in

concentration, sulfide contents and the $\delta^{34}S$ of residual sulfate should increase, as is observed at Hole U1413B (Figure 4). In that hole, sulfate decreases down the sediment column from 25 mM to levels below detection, while sulfide increases from concentrations below detection at top of the core to ~400 μM approaching the the SMT. Here, other chemical profiles respond to the high sulfate reduction such as the TOS, DOP, CRS, Fe-oxides and the ratio of pyrite to highly reactive iron. This is because the pulse of available pore water sulfide (from the reduction of sulfate) reacted with iron to form pyrites. At the same depth that sulfate concentration reaches a minimum and sulfide approaches its maximum measured levels in Hole U1413B, $\delta^{34}S\text{-}SO_4$ values rise to a peak of about +40‰. Recalling that average modern seawater $\delta^{34}S\text{-}SO_4$ ranges +17 to +22‰ (Paytan et al., 1998) and that biologically induced fractionation often drives $\delta^{34}S\text{-}SO_4$ to between +30 to +50‰ and less commonly up to around +70-72‰ (Goldhaber and Kaplan, 1980; Strauss 1997, Canfield and Teske, 1996, Wortmann et al., 2001), the fractionation observed in Hole U1413B is an unremarkable example of microbial sulfate reduction.

Data from Hole U1381C, however, are not as biogeochemically obvious. Not only does Hole U1381C lack sulfide accumulation as sulfate becomes depleted, but the $\delta^{34}S\text{-}SO_4$ measurements are very high (+75‰) at the peak and, puzzlingly, drop back down to the seawater average at ~100 mbsf. The drop in $\delta^{34}S$ corresponds to the depth at which sulfate, TOC, TOS, and calcium rise—in contrast to steady-state profiles—and the alkalinity drops. The increase of TOC at the bottom of the core from Hole U1381C is likely associated with higher sedimentation rate. Similarly,

Unit III of the core from Hole U1414A has higher TOC, which may be due to the rate of deposition (Expedition 344 Scientists, 2013b).

Hole U1414A is by far the most intriguing core with regard to measurements of $\delta^{34}S\text{-}SO_4$ and non-steady state conditions. Like the other two holes analyzed, U1414A also reflects removal of sulfate from pore waters through microbial sulfate reduction without appreciable sulfide accumulation (<4 μM H_2S). The first major question centers on the fate of the missing dissolved pore water sulfide given the likelihood that the fractionation of the sulfate pool in Hole U1414A is a consequence of biological sulfate reduction. Sulfide can be removed from pore waters via interactions with iron and other reactive metals (Berner, 1970; Berner 1984; Canfield et al., 1992; Huerta-Diaz and Morse, 1992). In case of sulfide removal by pyrite formation, there would be an accumulation of pyrite in the sediments (Raiswell and Canfield, 1998). Consistent with this pathway, measured pyrite sulfur (as CRS) in Holes U1381C, U1413B, and U1414A ranges from 0.1 to 1.8, 0.5 to 1.9, and 0.1 to 3.4 wt.%, respectively. These levels of pyrite abundance are moderate to high and aid in explaining the fate of pore water sulfide as they would have reacted with iron to form pyrite.

The second obvious question these data prompt is the magnitude of pore water sulfate fractionation ($\delta^{34}S\text{-}SO_4$) expressed within Holes U1381C and U1414A. The heaviest isotope ratio value for pore water sulfates previously measured is +135‰ ($\delta^{34}S\text{-}SO_4$ normalized to the V-CDT standard) (Rudnicki et al., 2001). The sample site featured in Rudnicki et al. (2001) is also along a subduction zone (the

Cascadia margin). There is a wealth of evidence that subduction zones, particularly those along continental margins, have increased rates of sulfate reduction in their sediments (Jørgensen, 1982; Canfield, 1991; Niewöhner et al., 1998; Fossing et al., 2000, Treude et al, 2005.) This increased sulfate reduction in these tectonically active regions may be linked to increased sediment deposition in along continental margins—as rate of deposition is closely linked to rates of sulfate reduction through rapid burial of labile organic matter (Berner, 1978). Sulfate delivery through fluid advection could also support microbial sulfate reduction in regions with related fractures, as is the case along the Costa Rica Margin (O'Hara et al., 1995; Torres et al., 1996; Ruppel and Kinoshita, 2000; Joye et al., 2004). Since we know that there is fluid flow in the Costa Rica margin and the $\delta^{34}S\text{-}SO_4$ in Hole U1414A is relatively constant (+60-70‰) for about 140 meters—corresponding to a stable sulfate concentration of 15mM—the fluid delivered to this portion of the sediment column may contain sulfate that is already isotopically heavy.

With the delivery of and abundance (~15 mM) of isotopically heavy sulfate (at +70‰) by way of fluid advection through the sediments of Hole U1414A, microbial reduction of sulfate need only drive the fractionation of the pore water sulfate heavier an additional 70‰ to achieve the unprecedented levels of $\delta^{34}S\text{-}SO_4$ found in our samples. The high $\delta^{34}S\text{-}SO_4$ of +135‰ in Rudnicki et al. (2001) from the Cascadia Margin also has isotopically heavy (ranging +40-100‰) pore water sulfate values down core of the heaviest value as well as remaining pore water sulfate of nearly 3 mM at the depth with the heaviest sulfate. Perhaps the Cascadia

Margin has upward advection of initially isotopically heavy sulfate pools thus requiring a smaller fractionation factor to result in such a high $\delta^{34}S\text{-}SO_4$ (+135‰). While the cause behind the initially high $\delta^{34}S\text{-}SO_4$ in the advection-transported fluids is unknown, it is possible that the systems in the Costa Rica Margin and Cascadia Margin are part of a yet to be established trend of sulfate pools being isotopically very heavy within the pore waters of subduction margins.

4.3 Rayleigh Model Applications and Interpretation

The high values for the sulfate isotope ratios found in Holes U1381C and the extreme $\delta^{34}S\text{-}SO_4$ value found in Hole U1414A from the Costa Rica margin are difficult to explain. In the previous section, a perfect storm of delivery of sulfate, microbial communities, and sulfide removal was proposed. However, since sulfate isotope ratios seen in our samples are unprecedented, it is important to understand what rate of reduction would be required and what the isotopic value of the original sulfate pool is in order to further characterize the conditions that result in such heavy $\delta^{34}S\text{-}SO_4$ values.

To determine the drivers of sulfate-S isotope fractionation, fractionation factors were calculated using a Rayleigh model. The model considered the highest pore water $\delta^{34}S$ values for sulfate in Holes U1414A and U1381C and explored different possible scenarios for seawater input and upward advection through the cores. Seawater input ($\delta^{34}S\text{-}SO_4$ =+20‰) via deep flow into the sediments is not very likely in Hole U1414 since the examined sediments are deeply buried and thus

will not be discussed, although it has been addressed in Table 2. Focus for that hole is instead placed on movement of fluids expelled during sediment compaction as this option is supported by previously mentioned research.

For the case of using modern seawater average of δ^{34}S-SO4= +20‰ as the input sulfate isotope value in Hole U1381C, an epsilon of -25 (or an α=0.975; see Equation 6 for the conversion from epsilon to alpha) would be required to achieve a $\delta^{34}S\text{-}SO_4$ value of +75‰. This alpha value matches those found by Rees (1973) for cultures of sulfate reducing bacteria that yielded a fractionation effect of +47‰ (in a closed system). Given the similar range of fractionator factors seen in previous works, the $\delta^{34}S\text{-}SO_4$ values in the pore waters of Hole U1381C are achieved with reasonably common sulfate reduction rates thereby proving a plausible explanation for the heavy sulfate isotope ratios at the site.

In Hole U1414A, modeling for an input sulfate pool with the isotope ratio found in modern seawater ($\delta^{34}S\text{-}SO_4$ =+20‰) yielded ε = -45 to -50 (α=0.995). When running the Rayleigh model for Hole U1414A considering the heavy and persistent (+65-70‰ across 190m) pool of sulfate the required fractionation factor to reach (+141‰) would range -40 to -50 (α=0.955). The alpha values for the modeled seawater input scenario is near that noted in Ohmoto and Lasaga (1982) for abiotically fractionated sulfate under simulated hydrothermal vent conditions of pH 2.1 and 100°C. Although the fractionation factor is a close match, it cannot be said that high-temperature abiotic fractionation must be the case in Hole U1414A. Hole U1414A yielded temperatures for the interval of isotopically heavy pore water

sulfate that did not exceed 20°C (as can be seen in the Appendix), nor does the pH range of 7.3-7.6 match the conditions of Ohmoto and Lasaga's simulated hydrothermal vent (Expedition 344 Scientists, 2013b). Although we can create a model matching our $\delta^{34}S\text{-}SO_4$ values, the fractionation factor needed to do so is quite high and not probable Rayleigh model used is the standard for closed systems, but a closed system isn't likely to have such high concentrations (4-5 mM) of heavy sulfate remaining. If we consider an open system with modern average seawater sulfate as the input, extreme fractionation needed (ε=70-90‰) to reach +141‰. However, if we consider the model when using an input value of $\delta^{34}S\text{-}SO_4$ =+65‰, the fractionation factor would not need to be so high. Not only is the fractionation factor lower than when modeling with seawater input (however, a low rate of sulfate reduction is still required) but this also allows for remaining sulfate in the pore waters. When starting with an isotopically heavy sulfate pool of 15mM sulfate, only about 70% of the available sulfate pool needs to be consumed during reduction to reach $\delta^{34}S\text{-}SO_4$ =+65‰ allowing for the remaining 4-5 mM of sulfate seen in Hole U1414A.

Rayleigh modeling is based on closed system reactions and thus must be used with caution in this study. The Costa Rica margin is without a doubt an open system. Nevertheless, use of Rayleigh modeling remains a powerful and often used approach to estimating fractionation factors. In Rudnicki et al. (2001), both Rayleigh modeling and an open system calculation were considered to find the fractionation factors of α=1.100 and α=1.077, respectively, for the $\delta^{34}S\text{-}SO_4$ values of +135‰. As

can be seen from the discrepancy in alpha values of 0.03, the agreement for the two approaches is quite strong. We can expect similar agreement in our case, and any differences would not change the fundamental conclusions of the study.

Although the heavy $\delta^{34}S\text{-}SO_4$ values observed in the Costa Rica Margin seem impossibly high at first, when taking into account the tectonically dynamic system, such values are achievable with a combination of low reduction rates and initially heavy sulfate pools. The fact that our consideration of upward advection fits best with the Rayleigh model to create the large (4-5mM) heavy (+135‰.) sulfate pool provides further evidence for previous suggestions of fluid transport within the deep sediments of the Costa Rica Margin. These findings also coincide with those for, the Cascadia Margin which is another subduction margin (Rudnicki, et al., 2001) with similar isotopic signals, making a case for a yet to be established trend and providing an explanation for heavy sulfate isotope signals found in future research. Another compelling implication is that our sulfate concentrations and isotope data indicate a sustained deep biosphere. Furthermore, the delivery of sulfate rich (and isotopically heavy) fluids to deep sediments in this subducting region is an example of the interplay between tectonic activity and biogeochemical cycling.

5. Conclusion

Among the most intriguing results of this research are the pore water sulfate isotope values, which are the heaviest on record from any location. Given that heavy sulfate isotope ratios (around +70‰) persist for tens of meters of depth below

heaviest $\delta^{34}S\text{-}SO_4$ and the tectonic activity within the sample site of the Costa Rica margin, it is likely that heavily fractionated fluids were introduced by flow within the sediments and further fractionated microbially to achieve the end $\delta^{34}S\text{-}SO_4$ values of up to +141‰. To further investigate the possibility that the heavy $\delta^{34}S\text{-}SO_4$ signal is biologically controlled, we applied Rayleigh modeling in an attempt to reproduce values observed in the Costa Rica margin sediments. Rayleigh modeling indicates that a high fractionation factor would be required (thus indicating a low rate of sulfate reduction) to reach the heavy pore water sulfate isotope ratios seen. The limitation of the Rayleigh model is that it is designed for application to closed systems. Given the tectonics of the region, running a Rayleigh model for a value consistent with upward advection not only provides a more reasonable fractionation factor than if the input $\delta^{34}S\text{-}SO_4$ was that of modern seawater but also provides further evidence of previously suggested fluid flow in the Costa Rica Margin.

A previous study yielded $\delta^{34}S\text{-}SO_4$ of up to +135‰ in the Cascadia Basin, a region tectonically similar to our sample site (Rudnicki et al., 2001). Considering that the Cascadia Basin and our study of the Costa Rica Margin share the characteristic of widespread fluid advection and are both accretionary prisms on subduction zones, it is possible that these data are representative of a trend that exists in the sediments of many subduction zones that awaits further recognition.

6. References

Abd-el-Malek, Y., Rizk, S.G., 1963. Bacterial sulphate reduction and the development of alkalinity. III. Experiments under natural conditions in the Wadi Natrûn. Journal of Applied Bacteriology 26, 20-26.

Allen, H.E., Fu, G., Deng, B., 1993. Analysis of acid-volatile sulfide (AVS) and simultaneously extracted metals (SEM) for the estimation of potential toxicity in aquatic sediments. Environmental Toxicology and Chemistry 12, 1-13.

Ammerman, C.B., Baker, D.H., Lewis, A.J. (Eds.), 1995. Bioavailability of nutrients in animals. Academic Press 1-441.

Berner, R.A., 1970. Sedimentary pyrite formation. American Journal of Science 268, 1-23.

Berner, R.A., 1978. Sulfate reduction and the rate of deposition of marine sediments. Earth and Planetary Science Letters 37, 492-498.

Berner, R.A., 1982. Burial of organic carbon and pyrite sulfur in the modern ocean: Its geochemical and environmental significance. American Journal of Science 282, 451-475.

Berner, R.A., 1985. Sulphate reduction, organic matter decomposition and pyrite formation. Philosophical Transactions of the Royal Society of London 315, 25-38.

Berner, R.A., 1989. Biogeochemical cycles of carbon and sulfur and their effect on atmospheric oxygen over Phanerozoic time. Paleogeography, Paleoclimatology, Paleoecology (Global and Planetary Change Section) 75, 97-122.

Berner, R.A., Baldwin, T., Holdren Jr., G.R., 1979. Authigenic iron sulfides as paleosalinity indicators. Journal of Sedimentary Petrology 49, 1345-1350.

Berner, R.A., Scott, M.R., Thomlinson, C., 1970. Carbonate alkalinity in the pore waters of anoxic marine sediments. Limnology and Oceanography 15, 544-549.

Böttcher, M.E., Khim, B.K., Suzuki, A., Gehre, M., Wortmann, U.G., Brumsack, H.J., 2004. Microbial sulfate reduction in deep sediments of the Southwest Pacific (ODP Leg 181, Sites 1119-1125): evidence from stable sulfur isotope fractionation and pore water modeling. Marine Geology 205, 249-260.

Bottrell, S.H., Raiswell, R., 2000. Sulphur isotopes and microbial sulphur cycling in sediments, in R.E. Riding and S.M. Awramik (Eds.), Microbial Sediments, Springer-Verlag Berlin Heidelberg, 96-104.

von Breymann, M.T., Brumsack, H., Emeis, K.C., 1992. Depositional and diagenetic behavior of barium in the Japan Sea, in: K. Pisciotto, J.C. Ingle, M.T. von Breymann and J. Barron (Eds.), Proceedings of the Ocean Drilling Program, Scientific Results, Vol. 128. ODP (Ocean Drilling Program), College Station Texas, 651-665.

Brosnan, J.T., Brosnan, M.E., 2006. The sulfur-containing amino acids: an overview. The Journal of Nutrition 136, 16365-16405.

Canfield, D.E., 1985. Sulfate reduction and oxic respiration in marine sediments: implications for organic carbon preservation in euxinic environments. Deep-Sea Research 36, 121-138.

Canfield, D.E., 1989. Reactive iron in marine sediments. Geochimica et Cosmochimica Acta 53, 619-632.

Canfield, D.E., 1991. Sulfate reduction in deep-sea sediments. American Journal of Science 291, 177-188.

Canfield, D.E., 1993. Organic matter oxidation in marine sediments, in: R. Wollast, F.T. Mackenzie and L. Chou (Eds.), Interactions of C, N, P and S in Biogeochemical Cycles and Global Change, Volume 4, Springer-Verlag Berlin Heidelberg, 333-363.

Canfield, D.E., 1994. Factors influencing organic carbon preservation in marine sediments. Chemical Geology 114, 315-329.

Canfield, D.E., Berner, R.A., 1987. Dissolution and pyritization of magnetite in anoxic marine sediments. Geochimica et Cosmochimica Acta 51, 645-659.

Canfield, D.E., Farquhar, J., Zerkle, A.L., 2010. High isotope fractionations during sulfate reduction in a low-sulfate euxinic ocean analog. Geology 38, 415-418.

Canfield, D.E., Raiswell, R., Bottrell, S.H., 1992. The reactivity of sedimentary iron minerals toward sulfide. American Journal of Science 292, 659-683.

Canfield, D.E., Raiswell, R., Westrich, J.T., Reaves, C.M., Berner, R.A., 1986. The use of chromium reduced inorganic sulfur in sediments and shales. Chemical Geology 54, 149-155.

Canfield, D.E., Teske, A., 1996. Late Proterozoic rise in atmospheric oxygen concentration inferred from phylogenetic and sulphur-isotope studies. Nature 382, 127-132.

Cline, J.D., 1969. Spectrophotometric determination of hydrogen sulfide in natural waters. Limnology and Oceanography 14, 454-458.

Cooper, A.J.L., 1983. Biochemistry of sulfur-containing amino acids. Annual Review of Biochemistry 52, 187-222.

Cornwell, J.C., Morse, J.W., 1987. The characterization of iron sulfide minerals in anoxic marine sediments. Marine Chemistry 22, 193-206.

Detmers, J., Brüchert, V., Habicht, K.S., Kuever, J., 2001. Diversity of sulfur isotope fractionations by sulfate-reducing prokaryotes. Applications of Environmental Microbiology 67, 888-894.

Expedition 344 Scientists, 2013a. Costa Rica Seismogenesis Project, Program A Stage 2 (CRISP-A2): sampling and quantifying lithologic inputs and fluid inputs and outputs of the seismogenic zone. IODP Preliminary Report, 344. Doi: 10.2204/iodp.pr.344.2013.

Expedition 344 Scientists, 2013b. Proceedings of the Integrated Ocean Drilling Program Volume 344, Principal Results. Doi: 10.2204/iodp.proc.344.101.2013

Ferdelman, T.G., 1988. The distribution of sulfur, iron, manganese, copper and uranium in a salt marsh sediment core as determined by a sequential extraction method. Masters thesis, University of Delaware.

Fossing, H., Ferdelman, T.G., Berg, P., 2000. Sulfate reduction and methane oxidation in continental margin sediments influenced by irrigation (South-East Atlantic off Namibia). Geochimica et Cosmochimica Acta 64, 897-910.

Fuller, C.W., Willett, S.D., Brandon, M.T., 2005. Formation of forearc basins and their influence on subduction zone earthquakes. Geology 34, 65-68.

Garrels, R.M., Christ, C.L., 1965. Solutions, Minerals and Equilibria. Harper & Row, New York.

Garrels, R.M., Lerman, A., 1984. Coupling of the sedimentary sulfur and carbon cycles; an improved model. American Journal of Science 284, 989-1007.

Goldhaber, M.B., Kaplan, I.R., 1974. The sulfur cycle. The Sea 5, 569-655.

Goldhaber, M.B., Kaplan, I.R., 1980. Mechanisms of sulfur incorporation and isotope fractionation during early diagenesis in sediments of the Gulf of California. Marine Chemistry 9, 95-143.

Goldhaber, M.B., Kaplan, I.R., 1982. Controls and consequences of sulfate reduction rates in recent marine sediments. Soil Science Society of America 119, 42-55.

Gröger, J., Franke, J., Hamer, K., Schulz, H.D., 2009. Quantitative recovery of elemental sulfur and improved selectivity in a chromium-reducible sulfur distillation. Geostandards and Geoanalytical Research 33, 17-27.

Habicht, K.S., Canfield, D.E., 1997. Sulfur isotope fractionation during bacterial sulfate reduction in organic-rich sediments. Geochimica et Cosmochimica Acta 61, 5352-5361.

Harrison, B.K., Zhang, H., Berelson, W., Orphan, V.J., 2009. Variations in archaeal and bacterial diversity associated with the sulfate-methane transition zone in continental margin sediments (Santa Barbara Basin, California). Applied and Environmental Microbiology 75, 1487-1499.

Hayes, J.M., 2004. An introduction to isotopic calculations. NOSAMS facility website [pdf at http://www.nosams.whoi.edu/research/staff_hayes.html]

Hensen, C., Wallmann, K., 2005, Methane formation at Costa Rica continental margin—constraints for gas hydrate inventories and cross-décollement fluid flow. Earth and Planetary Science Letters 236, 41-60.

Hoehler, T.M., Alperin, M.J., Albert, D.B., Martens, C.S., 1994. Field and laboratory studies of methane oxidation in an anoxic marine sediment: Evidence for a methanogen-sulfate reducer consortium. Global Biogeochemical Cycles 8, 451-463.

Holmkvist, L., Kamyshny Jr., A., Vogt, C., Vamvakopoulos, K., Ferdelman, T.G., Jørgensen, B.B., 2011. Sulfate reduction below the sulfate-methane transition in Black Sea sediments. Deep-Sea Research I 58, 493-504.

Holser, W.T., Kaplan, I.R., 1966. Isotope geochemistry of sedimentary sulfates. Chemical Geology 1, 93-135.

Horibe, Y., Endo, K., Tsubota, H., 1974. Calcium in the South Pacific, and its correlation with carbonate alkalinity. Earth and Planetary Science Letters 23, 136-140.

Huerta-Diaz, M.A., Morse, J.W., 1992. Pyritization of trace metals in anoxic marine sediments. Geochimica et Cosmochimica Acta 56, 2681-2702.

Ingall, E.D., Van Cappellen, P., 1990. Relation between sedimentation rate and burial of organic phosphorus and organic carbon in marine sediments. Geochimica et Cosmochimica Acta 54, 372-386.

Iversen, N., Jørgensen, B.B., 1985. Anaerobic methane oxidation rates at the sulfate-methane transition in marine sediments from Kattegat and Skagerrak (Denmark). Limnology and Oceanography 30, 944-955.

Jørgensen, B.B., 1977. The sulfur cycle of a coastal marine sediment (Limfjorden, Denmark). Limnology and Oceanography 22, 814-832.

Jørgensen, B.B., 1979. A theoretical model of the stable sulfur isotope distribution in marine sediments. Geochimica et Cosmochimica Acta 43, 363-372.

Jørgensen, B.B., 1982. Mineralization of organic matter in the sea bed-the role of sulphate reduction. Nature 296, 643-645.

Jørgensen, B.B., Fenchel, T., 1974. The sulfur cycle of a marine sediment model system. Marine Biology 24, 189-201.

Jørgensen, B.B., Nelsen, D.C., 2004. Sulfide oxidation in marine sediments: Geochemistry meets microbiology. Geological Society of America-Special Papers 379, 63-81.

Joye, S.B., Boetius A., Orcutt, B.N., Montoya, J.P., Schulz, H.N., Erickson, M.J., Lugo, S.K., 2004. The anaerobic oxidation of methane and sulfate reduction in sediments from Gulf of Mexico cold seeps. Chemical Geology 205, 219-238.

Kahn, L.M., Silver, E.A., Orange, D., Kochevar, R., McAdoo, B., 1996. Surficial evidence of fluid expulsion from the Costa Rica Accretionary Prism. Geophysical Research Letters 23, 887-890.

Kaplan, I.R., Rittenberg, S.C., 1964. Microbiological fractionation of sulphur isotopes. 34, 195-212.

Kendall, C., Caldwell, E.A., 1998. Fundamentals of Isotope Geochemistry. In: Kendall, C., McDonnell, J.J. (Eds.), Isotope tracers in catchment hydrology. Elsevier Science B.V., 51-89.

Keys, A., Christensen, E.H., Krogh, A., 1935. The organic metabolism of sea-water with special reference to the ultimate food cycle in the sea. Journal of the Marine Biological Association of the United Kingdom (New Series) 20, 181-196.

Knab, N.J., Dale, A.W., Lettman, K., Fossing, H., Jørgensen, B.B., 2008. Thermodynamic and kinetic control on anaerobic oxidation of methane in marine sediments. Geochimica et Cosmochimica Acta 72, 3746-3757.

Kvenvolden, K.A., 1988. Methane hydrate – A major reservoir of carbon in the shallow geosphere? Chemical Geology 71, 41-51.

Leavitt, W.D., Halevy, I., Bradley, A.S., Johnston, D.T., 2013. Influence of sulfate reduction rates on the Phanerozoic sulfate isotope record. PNAS 110, 11244-11249.

Li, X., Taylor, G.T., Astor, Y., Scranton, M.I., 2008. Relationship of sulfur speciation to hydrographic conditions and chemoautotrophic production in the Cariaco Basin. Marine Chemistry 112, 53-64.

Luff, R., Wallmann, K., 2003. Fluid flow, methane fluxes, carbonate precipitation and biogeochemical turnover in gas hydrate-bearing sediments at Hydrate Ridge, Cascadia Margin: Numerical modeling and mass balances. Geochimica et Cosmochimica Acta 67, 3403-3421.

Martens, C.S., Klump, J.V., 1984. Biogeochemical cycling in an organic-rich coastal marine basin 4. An organic carbon budget for sediments dominated by sulfate reduction and methanogenesis. Geochimica et Cosmochimica 48, 1987-2004.

Niewöhner, C., Hensen, C., Kasten, S., Zabel, M., Schulz, H.D., 1998. Sulfate reduction completely mediated by anaerobic methane oxidation in sediments of the upwelling area off Namibia. Geochimica et Cosmochimica Acta 62, 455-464.

O'Flaherty, V., Mahoney, T., O'Kennedy, R., Colleran, E., 1998. Effect of pH on growth kinetics and sulphide toxicity thresholds of a range of methanogenic, syntrophic and sulphate-reducing bacteria. Process Biochemistry 33, 555-569.

Ohmoto, H., Lasaga, A.C., 1982. Kinetics of reactions between aqueous sulfates and sulfides in hydrothermal systems. Geochimica et Cosmochimica Acta 46, 1727-1745.

O'Hara, S.C.M., Dando, P.R., Schuster, U., Bennis, A., Boyle, J.D., Chui, F.T.W., Hatherell, T.V.J., Niven, S.J., Taylor, L.J., 1995. Gas seep induced interstitial water circulation: observations and environmental implications. Continental Shelf Research 15, 931-948.

Orcutt, B.N., Sylvan J.B., Knab, N.J., Edwards, K.J., 2011. Microbial ecology of the dark ocean above, at, and below the seafloor. Microbiology and Molecular Biology Reviews, June 2011, 361-422.

Oremland, R.S., Taylor, B.F., 1978. Sulfate reduction and methanogenesis in marine sediments. Geochimica et Cosmochimica Acta 42, 209-214.

Paytan, A., Kastner, M., Campbell, D., Thiemens, M.H., 1998. Sulfur isotopic composition of Cenozoic seawater sulfate. Science 282, 1459-1462.

Poulton, S.W., Canfield, D.E., 2005. Development of a sequential extraction procedure for iron: implications for iron partitioning in continentally derived particulates. Chemical Geology 214, 209-221.

Raiswell, R., Buckley, F., Berner, R.A., Anderson, T.F. 1988. Degree of pyritization of iron as a paleoenvironmental indicator of bottom-water oxygenation. Journal of Sedimentary Research 58, 812-819.

Raiswell, R., Canfield, D.E., 1998. Sources of iron for pyrite formation in marine sediments. American Journal of Science 298, 219-245.

Raiswell, R., Canfield, D.E., Berner, R.A., 1994. A comparison of iron extraction methods for the determination of degree of pyritization and the recognition of iron-limited pyrite formation. Chemical Geology 111, 101-110.

Raiswell, R., Vu, H.P., Brinza, L., Benning L.G., 2010. The determination of labile Fe in ferrihydrite by ascorbic acid extraction: Methodology, dissolution kinetics and loss of solubility with age and de-watering. Chemical Geology 278, 70-79.

Redfield, A.C., 1958. The biological control of chemical factors in the environment. American Scientist 46, 230A, 205-221.

Reeburgh, W.S., 1976. Methane consumption in Cariaco Trench waters and sediments. Earth and Planetary Science Letters 28, 337-344.

Rees, C.E., 1973. A steady-state model for sulphur isotope fractionation in bacterial reduction processes. Geochimica et Cosmochimica Acta 37, 1141-1162.

Rees, C.E., Jenkins, W.J., Monster, J., 1978. The sulphur isotopic composition of ocean water sulphate. Geochimica et Cosmochimica Acta 42, 377-381.

Refait, P., Génin, J.-M.R., 1997, The mechanisms of oxidation of ferrous hydroxychloride β-$Fe_2(OH)_3Cl$ in aqueous solution: The formation of akagenéite vs goethite. Corrosion Science 39, 539-553.

Reis, M.A.M., Almeida, J.S., Lemos, P.C., Carrondo, M.J.T., 1992. Effect of hydrogen sulfide on growth of sulfate reducing bacteria. Biotechnology and Bioengineering 40, 593-600.

Reisner, D.B., 1956. Sulfur-containing Amino Acids. Journal of the American Chemical Society 78, 2132-2135.

Rickard, D., Morse, J.W., 2005. Acid volatile sulfide (AVS). Marine Chemistry 97, 141-197.

Riedinger, N., Kasten, S., Gröger, J., Franke, C., Pfeifer, K., 2006. Active and buried authigenic barite fronts in sediments from the Eastern Cape Basin. Earth and Planetary Science Letters 241, 876-887.

Riedinger, N., Strasser, M., Harris, R.N., Klockgether, G., Lyons, T.W., Screaton, E.J., 2015. Deep subsurface carbon cycling in the Nankai Trough (Japan) – Evidence of tectonically induced stimulation of a deep microbial biosphere. Geochemistry, Geophysics, Geosystems 16, 3257-3270.

Ritger, S., Carson, B., Suess, E., 1987. Methane-derived authigenic carbonates formed by subduction-induced pore-water expulsion along Oregon/Washington margin. Geological Society of America Bulletin 98, 147-156.

Rudnicki, M.D., Elderfield, H., Spiro, B., 2001. Fractionation of sulfur isotopes during bacterial sulfate reduction at elevated temperatures. Geochimica et Cosmochimica Acta 65, 777-789.

Ruppel, C., Kinoshita, M., 2000. Fluid, methane and energy flux in an active margin gas hydrate province, offshore Costa Rica. Earth and Planetary Science Letters 179, 153-165.

Shen, X., Carlström, M., Borniquel, S., Jädert, C., Kevil, C.G., Lundberg, J.O., 2013. Microbial regulation of host hydrogen sulfide bioavailability and metabolism. Free Radical Biology and Medicine 60, 195-200.

Shipley, T.H., Houston, M.H., Buffler, R.T., Shaub, J., McMillen, K.J., Ladd, J.W., Worzel, J.L., 1979. Seismic evidence for widespread possible gas hydrate horizons on continental slopes and rises. American Association of Petroleum Geologists Bulletin 63, 2204-2213.

Sim, M.S., Bosak, T., Ono, S., 2011. Large sulfur isotope fractionation does not require disproportionation. Science 333, 74-77.

Stavenhagen, A.U., Flueh, E.R., Ranero, C., McIntosh, K.D., Shipley, T., Leandro, G., Schulze, A., Dañobeitia, J.J., 1998. Seismic wide-angle investigations in Costa Rica: A crustal velocity model from the Pacific to the Caribbean Coast. ZBL, Geological Paläontologie Part I, 393-408.

Strauss, H., 1997. The isotopic composition of sedimentary sulfur through time. Palaeogeography, Palaeoclimatology, Palaeoecology 132, 97-118.

Szabo, A., Tudge, A., Macnamara, J., Thode, H.G., 1950. The distribution of S^{34} in nature and the sulfur cycle. Science 28, 464-465.

Thode, H.G., Monster, J., Dunford, H.B., 1961. Sulphur-isotope geochemistry. Geochimica et Cosmochimica Acta 25, 159-174.

Thode, H.G., 1970. Sulfur isotope geochemistry and fractionation between coexisting sulfide minerals. Mineralogical Society of America- Special Papers 3, 133-144.

Torres, M., Brumsack, H.J., Bohrmann, G., Emeis, K.C., 1996. Barite front in continental margin sediments: A new look at barium remobilization in the zone of sulfate reduction and formation of heavy barites in diagenetic fronts. Chemical Geology 127, 125-139.

Toth, D.J., Lerman, A., 1977. Organic matter reactivity and sedimentation rates in the ocean. American Journal of Science 277, 265-285.

Treude, T., Niggemann, J., Kallmeyer, J., Wintersteller, P., Schubert, C.J., Boetius, A., Jørgensen, B.B., 2005. Anaerobic oxidation of methane and sulfate reduction along the Chilean continental margin. Geochimica et Cosmochimica Acta 69, 2767-2779.

Tsunogai, S., Watanabe, Y., 1981. Calcium in the North Pacific water and the effect of organic matter on the calcium-alkalinity relation. Geochemical Journal 15, 95-107.

Tsunogai, S., Yamahata, H., Kudo, S., Saito, O., 1973. Calcium in the Pacific Ocean. Deep-Sea Research 20, 717-726.

Viollier, E., Inglett, P.W., Hunter, K., Roychoudhury, A.N., Van Cappellen, P., 2000. The ferrozine method revisited: Fe(II)/Fe(III) determination in natural waters. Applied Geochemistry 15, 785-790.

Werne, J.P., Lyons, T.W., Hollander, D.J., Formolo, M.J., Sinninghe Damsté, J.S., 2003. Reduced sulfur in euxinic sediments of the Cariaco Basin: sulfur isotope constraints on organic sulfur formation. Chemical Geology 195, 159-179.

Westrich, J.T., Berner, R.A., 1984. The role of sedimentary organic matter in bacterial sulfate reduction: The G model tested. Limnology and Oceanography 29, 236-249.

Wolf-Gladrow, D.A., Zeebe, R.E., Klaas, C., Körtzinger, A., Dickson, A.G., 2007. Total alkalinity: The explicit conservative expression and its application to biogeochemical processes. Marine Chemistry 106, 287-300.

Wortmann, U.G., Bernasconi, S.M., Böttcher, M.E., 2001. Hypersulfidic deep biosphere indicates extreme sulfur isotope fractionation during single-step microbial sulfate reduction. Geology 29, 647-650.

7. Appendix

Fig. 10 Temperature profile for Hole U1414A Profile for the temperature had been measured for four points (black dots) and modeled for the remainder of the hole (black solid line). Adapted from Expedition 344 Scientists, 2013b.

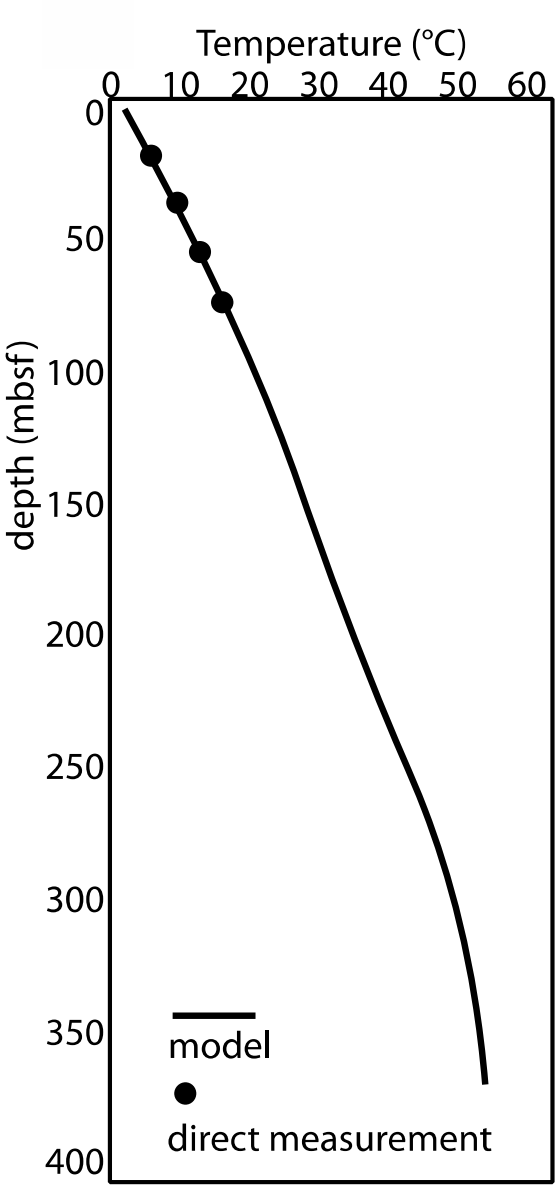

Table 3 Samples and depths A compiled list of the samples used in this study along with their depths (Expedition 344 Scientists, 2013b).

Sample ID U1414A	Mean depth (mbsf)	Sample ID U1413B	Mean depth (mbsf)	Sample ID U1381C	Mean depth (mbsf)
U1414A 1H1	0.5565	U1413B 1H1	1.4395	U1381C 1H1	1.489
U1414A 2H1	3.1985	U1413B 1H2	2.9275	U1381C 1H3	7.445
U1414A 2H3	5.8915	U1413B 1H3	4.4175	U1381C 1H5	4.467
U1414A 2H5	8.5835	U1413B 1H4	5.5075	U1381C 1H5	4.467
U1414A 3H2	14.008	U1413B 1H5	6.2035	U1381C 2H4	13.795
U1414A 3H5	17.99	U1413B 2H1	7.986	U1381C 2H6	16.642
U1414A 4H2	23.56	U1413B 2H2	9.42	U1381C 3H2	20.432
U1414A 4H5	27.643	U1413B 2H3	10.853	U1381C 3H4	23.265
U1414A 5H2	33.058	U1413B 2H4	12.287	U1381C 3H6	26.098
U1414A 5H5	37.117	U1413B 2H5	13.72	U1381C 4H3	31.349
U1414A 6H2	42.7115	U1413B 2H6	14.843	U1381C 4H5	34.182
U1414A 6H5	47.0135	U1413B 2H6	15.034	U1381C 5H3	40.885
U1414A 7H2	52.226	U1413B 2H6	15.154	U1381C 5H6	45.152
U1414A 7H5	56.535	U1413B 2H7	15.321	U1381C 6H3	50.419
U1414A 8H2	61.7515	U1413B 2H7	15.512	U1381C 6H6	54.682
U1414A 9H2	71.23	U1413B 2H7	15.703	U1381C 7H3	59.85
U1414A 9H5	75.549	U1413B 2H7	15.87	U1381C 7H6	63.956
U1414A 10H2	80.742	U1413B 3H1	16.21	U1381C 7H6	64.099
U1414A 10H5	85.078	U1413B 3H1	16.3845	U1381C 8H3	69.381
U1414A 11H2	90.2745	U1413B 3H2	17.965	U1381C 8H6	73.663
U1414A 11H5	94.6585	U1413B 3H3	19.296	U1381C 9H3	78.918
U1414A 12H2	99.734	U1413B 3H4	20.592	U1381C 9H6	83.092
U1414A 12H5	104.057	U1413B 3H5	21.906	U1381C 9H6	83.236
U1414A 13H2	109.3185	U1413B 3H6	23.219	U1381C 10H	86.976
U1414A 13H5	113.7725	U1413B 3H7	24.532	U1381C 10H	88.414
U1414A 14H2	118.73	U1413B 3H8	25.32	U1381C 10H	91.29
U1414A 15H2	128.2745			U1381C 10H	92.727
U1414A 15H5	132.6585			U1381C 11H	95.024
U1414A 16H2	137.485			U1381C 11H	96.448
U1414A 16H5	141.875			U1381C 11H	97.871
U1414A 17H4	150.251			U1381C 11H	100.719
U1414A 18H5	159.4095			U1381C 11H	102.142
U1414A 19H3	166.279				
U1414A 19H6	170.532				
U1414A 20H2	174.4975				
U1414A 20H5	178.9755				
U1414A 21H3	185.1345				
U1414A 22H6	198.875				
U1414A 38R1	327.44				
U1414A 38R2	328.39				